European Reviews of Chemical Research

Has been issued since 2014. ISSN 2312-7708, E-ISSN 2413-7243
2015. Vol.(6). Is. 4. Issued 4 times a year

The journal is registered by Federal Service for Supervision of Mass Media, Communications and Protection of Cultural Heritage (Russian Federation). Registration Certificate **ПИ № ФС77-57042** 25.02.2014.

Journal is indexed by: **CrossRef** (UK), **Electronic scientific library** (Russia), **Journal Index** (USA), **Open Academic Journals Index** (Russia), **ResearchBib** (Japan), **Scientific Indexing Services** (USA)

All manuscripts are peer reviewed by experts in the respective field. Authors of the manuscripts bear responsibility for their content, credibility and reliability.

Editorial board doesn't expect the manuscripts' authors to always agree with its opinion.

Postal Address: 26/2 Konstitutcii, Office 6
354000 Sochi, Russian Federation

Website: http://ejournal14.com/en/index.html
E-mail: evr2010@rambler.ru
Founder and Editor: Academic Publishing House *Researcher*

Passed for printing 15.12.15.
Format 21 × 29,7/4.

Headset Georgia.
Ych. Izd. l. 5,1. Ysl. pech. l. 5,8.
Order № 106.

European Reviews of Chemical Research

2015
Is. 4

Европейские обзоры химических исследований

2015

№ 4

Европейские обзоры химических исследований

Издается с 2014 г. ISSN 2312-7708, E-ISSN 2413-7243
2015. № 4 (6). Выходит 4 раза в год.

Журнал зарегистрирован Федеральной службой по надзору в сфере массовых коммуникаций, связи и охраны культурного наследия (Российская Федерация). Свидетельство о регистрации средства массовой информации **ПИ № ФС77-57042** 25.02.2014.

Журнал индексируется в: **CrossRef** (Великобритания), **Journal Index** (США), **Научная электронная библиотека** (Россия), **Open Academic Journals Index** (Россия), **ResearchBib** (Япония), **Scientific Indexing Services** (США)

Адрес редакции: 354000, Российская Федерация, г. Сочи, ул. Конституции, д. 26/2, оф. 6
Сайт журнала: **http://ejournal14.com**
E-mail: **evr2010@rambler.ru**

Учредитель и издатель: ООО «Научный издательский дом "Исследователь"» - Academic Publishing House *Researcher*

Подписано в печать 15.12.15.
Формат 21 × 29,7/4.

Гарнитура Georgia.
Уч.-изд. л. 5,1. Усл. печ. л. 5,8.
Заказ № 106.

C O N T E N T S

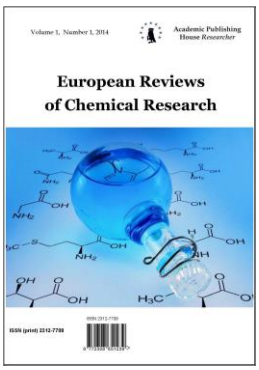

Published in the Russian Federation
European Reviews of Chemical Research
Has been issued since 2014.
ISSN: 2312-7708
E-ISSN: 2413-7243
Vol. 6, Is. 4, pp. 192-211, 2015

DOI: 10.13187/ercr.2015.6.192
www.ejournal14.com

UDC 541.64:574.24:553.08

The Methods of non-equilibrium Spectrum (NES) and Differential non-equilibrium Spectrum (DNES) in Studying the Interaction of Carbonaceous Mineral Shungite and Aluminosilicate Mineral Zeolite with Water

[1] Ignat Ignatov
[2] Oleg Mosin

[1] The Scientific Research Center of Medical Biophysics (SRC MB), Bulgaria
Professor, D. Sc., director of SRC MB
1111, Sofia, N. Kopernik street, 32
E-mail: mbioph@dir.bg
[2] Moscow State University of Applied Biotechnology, Russian Federation
Senior research Fellow of Biotechnology Department, Ph. D. (Chemistry)
103316, Moscow, Talalihina ulitza, 33
E-mail: mosin-oleg@yandex.ru

Abstract

The mathematical model of interaction with water the amorphous, uncrystallized, fullerene analogous carbon containing natural mineral shungite (Zazhoginskoe deposit, Karelia, Russia) and micro-porous alumosilicate mineral zeolite (Most, Bulgaria) was established. There are submitted data on the nanostructure and structural properties of these minerals, obtained with using the elemental analysis, transmission electron microscopy (TEM-method) and IR-spectroscopy. For evaluation of the mathematical model of interaction of these minerals with water, the methods of non-equilibrium spectrum (NES) and differential non-equilibrium spectrum (DNES) of water were applied. The values of average energy ($\Delta E_{H...O}$) of hydrogen H...O-bonds among H_2O molecules in water samples after the treatment of shungite and zeolite with water was measured at -0,1137 eV for shungite and -0,1174 eV for zeolite. The calculation of $\Delta E_{H...O}$ for shungite with using the DNES method compiles +0,0025±0,0011 eV and for zeolite -1,2±0,0011 eV. It was demonstrated a regularity of change of energy of hydrogen bonds between H_2O molecules in the process of water treatment by shungite and zeolite with a statistically reliable increase of local maximums in DNES-spectra.

Keywords: shungite, zeolite, nanostructure, fullerens, IR, NES, DNES

Introduction

Shungite and zeolite – the minerals refer to new generation of natural mineral sorbents (NMS). Shungite is an intermediate form between the amorphous carbon and the graphite crystal, containing carbon (30 %), silica (45 %), and silicate mica (about 20 %) [1]. The schungite carbon is a fossilized organic material of the sea bottom Precambrian sediments of high level of carbonization containing the fullerene-like regular structures. Shungite got its name after the village of Shunga in Karelia (Russian Federation), located on the shore of Onezhskoe Lake, where is

located the only one mineral Zazhoginsky deposit of shungites on the territoty of the Russian Federation. The total shungite researves of Zazhoginsky deposit amount to approximately 35 million tons of shungite. The plant production capacity for the mining and processing of shungite makes up 200 thousand tons of shungite per year.

Zeolites are the alumosilicate members of the family of microporous solids known as "molecular sieves", named by their ability to selectively sort molecules based primarily on a size exclusion process. The natural zeolites formed when the volcanic rocks and ash layers reacted with alkaline groundwater. Zeolites also crystallize in post-depositional environments over periods ranging from thousands to millions of years in shallow marine basins. The naturally occurring zeolites are rarely pure and are contaminated to varying degrees by other minerals, metals, quarts, or other zeolites. For this reason, naturally occurring zeolites are excluded from many important commercial applications where uniformity and purity are essential.

As natural minerales shungite and zeolite have unusually broad scope of application in industry. Shungite was used initially, mainly as a filler and substitute of the carbon coal coke (fuel) in blast furnace production of high-silicon cast iron, in ferroalloys melting, in the production of non-stick heat-resistant paints and coatings, and as filler in rubber production. Subsequently there were discovered other new valuable properties of shungite – adsorptional, bactericidal, catalytic, reduction-oxidation properties, as well as the ability of sungite minerals to screen off electromagnetic and radio radiations. These properties have made the use of shungite in various branches of science, industry and technology, for creating on its basis a variety of new nanotechnological materials with nano-molecular structure [2]. On the basis of shuntite has been created new conductive paints, fillers for plastic materials, rubber and carbon black substitutes, composite materials, concrete, bricks, stuccoing plasters, asphalts, as well as materials having bactericidal activity and materials shilding off the radio and electromagnetic radiation. The adsorption, catalytic, and reduction-oxydation properties of shungite favored its use in water treatment and water purification technologies [3], i.g. in treatment of sewage waters from many organic and inorganic substances (heavy metals, ammonia, organochlorine compounds, petroleum, phenols, surfactants, etc.). Moreover, shungite has a strongly marked biological activity and bactericidal properties.

Zeolites as shungites are widely used in industry as a desiccant of gases and liquids [4], for treatment of drinking and sewage water from heavy metals, ammonia, phosphorus [5], as a catalyst in petrochemical industry (shungite), for benzene extraction and for extracting of radionuclides in nuclear reprocessing. They are also used in medicine as nutritional supplements having antioxidant properties.

A wide range of properties of shungite and zeolite defines the search for new areas of industrial application of these minerals in science and technology that contributes to a deeper study of the structure with using the modern analytical methods. This research paper deals with investigation of the structural properties of shungite and zeolite and evaluation of the mathematical model of interaction of these minerals with water.

Material and methods

Material

The study was performed with samples of shungite obtained from Zazhoginsky deposit (Karelia, Russia) and zeolite (Most, Bulgaria). Samples were taken and analyzed in solid samples according to National standard of the Russian Federal Agency of Technical Regulation and Metrology. Samples were put into 100 cm^3 hermetically sealed glass tubes after being washed in dist. H_2O and dried in crucible furnace, and homogenized in homogenizer by mechanical grinding. For the decomposition of the shungite samples a system of microwave decomposition was used. Other methods of samples processing were watching with dist. H_2O, drying, and homogenization on cross beater mill Retsch SK100 ("Retsch Co.", Germany) and Pulverisette 16 ("Fritsch GMBH", Germany).

Analytical methods

The analytical methods were accredited by the Institute of Geology of Ore Deposits, Petrography, Mineralogy, and Geochemistry (Russian Academy of Sciences). Samples were treated by various methods as ICP-OES, GC, and SEM.

Gas-chromatography

Gas-chromatography (GC) was performed at Main Testing Centre of Drinking Water (Moscow, the Russian Federation) on Kristall 4000 LUX M using Chromaton AW-DMCS and Inerton-DMCS columns (stationary phases 5 % SE-30 and 5 % OV-17), equipped with flame ionization detector (FID) and using helium (He) as a carrier gas.

Inductively coupled plasma optical emission spectrometry (ICP-OES)

The mineral composition of shungite was studied by inductively coupled plasma optical emission spectrometry (ICP-OES) on Agilent ICP 710-OES (Agilent Technologies, USA) spectrometer, equipped with plasma atomizer (under argon stream), Mega Pixel CCD detector, and 40 MHz free-running, air-cooled RF generator, and Computer-optimized echelle system: the spectral range at 167–785 nm; plasma gas: 0–22,5 l/min in 1,5 l/min; power output: 700–1500 W in 50 W increments.

Elemental analysis

The total amount of carbon (C_{total}) in shungite was measured according to the ISO 29541 standard using elemental analyzer CHS-580 ("Eltra GmbH", Germany), equipped with electric furnace and IR-detector by combustion of 200 mg of solid homogenized sample in a stream of oxygen at the temperature +1500 ^{o}C.

Transmission electron microscopy

The structural studies were carried out with using transmission electron microscopy (TEM) on JSM 35 CF (JEOL Ltd., Korea) device, equipped with X-ray microanalyzer "Tracor Northern TN", SE detector, thermomolecular pump, and tungsten electron gun (Harpin type W filament, DC heating); working pressure: 10^{-4} Pa (10^{-6} Torr); magnification: 300000, resolution: 3,0 nm, accelerating voltage: 1–30 kV; sample size: 60–130 mm.

IR-spectroscopy

IR-spectra of shungite were registered on Fourier-IR spectrometer Brucker Vertex ("Brucker", Germany) (a spectral range: average IR – 370–7800 cm^{-1}; visible – 2500–8000 cm^{-1}; the permission – 0,5 cm^{-1}; accuracy of wave number – 0,1 cm^{-1} on 2000 cm^{-1}).

NES- and DNES-methods

NES- and DNES-methods were used for the estimation of energy of hydrogen bonds of shungite zeolite solutions in water in order to evaluate the mathematical model of interaction of these minerals with water. The device measured the angle of evaporation of water drops from 72^{o} to 0^{o}. As the main estimation criterion was used the average energy ($\Delta E_{H...O}$) of hydrogen O...H-bonds between individual H_2O molecules in aqueous samples. NES-and DNES spectra of shungite and zeolite solutions in water were measured in the range of the energy of hydrogen bonds 0,08–0,387 eV or wave lengths λ = 8,9–13,8 μm with using a specially designed computer program.

Results and Discussion

The composition and the structure of shungite and zeolite

According to the last structural studies shungite is a metastable allotropic form of carbon with high level of carbonization (carbon metamorhism), being on prior to graphite stage of coalification [6]. Along with carbon the shungite, obtained from Zazhoginsky deposit in Karelia (Russian Federation) contains SiO_2 (57,0 %), TiO_2 (0,2 %), Al_2O_3 (4,0 %), FeO (0,6 %), Fe_2O_3 (1,49 %), MgO (1,2 %), MnO (0,15 %), K_2O (1,5 %), S (1,2 %) (Table 1). The product obtained after the thermal firing of shungite (shungizite) at +1200...+1400 ^{o}C contains in small amounts V (0,015 %),

B (0,004 %), Ni (0,0085 %), Mo (0,0031 %), Cu (0,0037 %), Zn (0,0067 %), Co (0,00014 %) As (0,00035 %), Cr (0,72 %), Zn (0,0076 %) and other elements (Table 2).

Table 1: The chemical composition of shungites from Zazhoginsky deposit (Karelia, Russian Federation), in % (w/w)

№	Chemical component	Content, % (w/w)
1	C	30,0
2	SiO_2	57,0
3	TiO_2	0,2
4	Al_2O_3	4,0
5	FeO	0,6
6	Fe_2O_3	1,49
7	MgO	1,2
8	MnO	0,15
9	CaO	0,3
10	Na_2O	0,2
11	K_2O	1,5
12	S	1,2
13	H_2O	1,7

Table 2: The chemical composition of shungite after the heat treatment at +1400 ^oC

№	Chemical component	Content, % (w/w)
1	C	26,25
2	SiO_2	3,45
3	TiO_2	0,24
4	Al_2O_3	3,05
5	FeO	0,32
6	Fe_2O_3	1,01
7	MgO	0,56
8	MnO	0,12
9	CaO	0,12
10	Na_2O	0,36
11	K_2O	1,23
12	S	0,37
14	P_2O_3	0,03
15	Ba	0,32
16	B	0,004
17	V	0,015
18	Co	0,00014
19	Cu	0,0037
20	Mo	0,0031
21	As	0,00035
22	Ni	0,0085
23	Pb	0,0225
24	Sr	0,001
26	Cr	0,0072
26	Zn	0,0067
27	H_2O	0,78
28	Calcination (burning) losses	32,78

In comparison with shungite, zeolite comprises a microporous crystalline aluminosilicate mineral commonly used as a commercial adsorber, the three-dimensional framework of which is

formed by the tetrahedra – $[AlO_4]^{2-}$ and $[SiO_4]^{2-}$ linking to each other via the vertices [7]. Each tetrahedron $[AlO_4]^{2-}$ creates a negative charge of the carcasses compensated by cations (H^+, Na^+, K^+, Ca^{2+}, NH_4^+, etc.), which in most cases capable of cation exchange in water solutions. In between the crystalline framework are arranged the hydrated positive ions of alkali and alkaline earth metals – sodium, potassium, calcium, less magnesium, barium, strontium, compensating the carcass charge and water molecules. The tetrahedrons $[AlO_4]^{2-}$ and $[SiO_4]^{2-}$ form the secondary structural units, such as six-membered rings, five-membered rings, truncated octahedra, etc. (Fig. 1). As a result the zeolite framework composes the interacting channels and cavities forming a porous structure with a pore size of 0,3–1,0 nm. An average crystal size of the zeolite may range from 0,5 to 30 μm.

The empirical formula of zeolite can be represented as follows:

$$M_{2/n}O \cdot Al_2O_3 \cdot \gamma SiO_2 \cdot wH_2O,$$

where n – the cationic charge (n = 1–2); γ – the molar ratio of oxides of silicon and aluminum in the zeolite framework, indicating the amount of cation exchange positions in the structure (y = 2–∞); w – the amount of water.

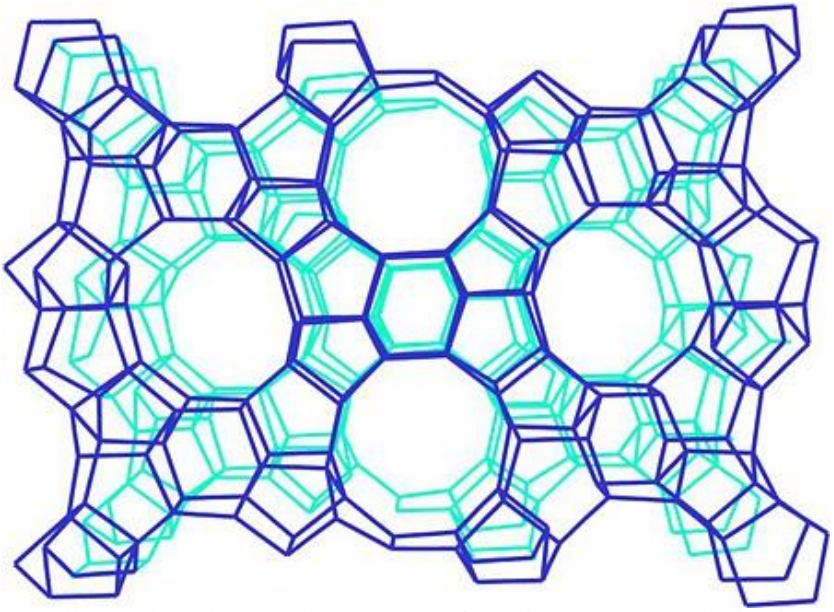

Figure 1. The three-dimensional crystal structure of zeolite ZSM-5 with the formula $Na_2[Al_2Si_{96-n}O_{192}]\cdot 16H_2O$ (n = 3–5), cell size – 0,51–0,56

Currently, there are known more than 30 varieties of natural zeolites, but only some of them form large deposits (80 % of concentrates) suitable for industrial processing. The most common natural zeolites:

• Chabazite $(Ca,Na_2)[Al_2Si_4O_{12}]\cdot 6H_2O$ with cell size 0,37–0,50 nm;

• Mordenite $(Ca,Na_2,K_2)[Al_2Si_{10}O_{24}]\cdot 7H_2O$ with cell size 0,67–0,70 nm;

• Klinoptilomite $(Na_2,K_2,Ca)[Al_2O_3\cdot 10SiO_2]\cdot 8H_2O$ with cell size 0,75–0,82 nm.

The synthetic zeolites have the composition and the crystal structure similar to the natural zeolites:

• Zeolites of A-type A are represended by low silicate forms: in them the ratio $Sio_2:Al_2o_3$ does not exceed 2,0;

• Zeolites of X-type have the ratio $Sio_2:Al_2o_3$, which varies from 2,2 to 3,3;

• Zeolites of Y-type are characterized by the ratio of $Sio_2:Al_2o_3$ in the range of 3,1 to 6,0. By increasing this ratio the acid resistance of zeolites increases. The pore sizes define the selectivity which varies from 0,0003 to 0,0009 μm.

The composition of zeolite from Most (Bulgaria) is analogous to that of shungite (Table 3), except for carbon which does not occur in zeolite. The amounts of core elements (SiO_2, TiO_2, Al_2O_3, FeO, Fe_2O_3, MgO, CaO, Na_2O, K_2O, S) constituting this mineral differ from that of shungite: their content is higher than that of shungite, except for TiO_2 and K_2O, the contents of which in zeolite were dicreased (Table 3). The content of microelements as V (0,0272 %), Co (0,0045 %), Cu (0,0151 %), Mo (0,0012 %), As (0,0025 %), Ni (0,0079 %), Zn (0,1007 %), Zn (0,1007 %) was somewhat increased in zeolite, while the content of Ba (0,0066 %) and Cr (0,0048 %) was increased (Table 3).

Table 3: The chemical composition of zeolite (Most, Bulgaria), in % (w/w)

№	Chemical component	Content, % (w/w)
1	SiO_2	22,14
2	TiO_2	0,01
3	Al_2O_3	17,98
4	FeO	23,72
5	Fe_2O_3	1,49
6	MgO	14,38
7	MnO	0,61
8	CaO	0,36
9	Na_2O	0,5
10	K_2O	0,4
11	S	0,32
12	P_2O_5	0,06
13	Ba	0,0066
14	V	0,0272
15	Co	0,0045
17	Cu	0,0151
18	Mo	0,0012
19	As	0,0025
20	Ni	0,0079
21	Pb	0,0249
22	Sr	0,0021
23	Cr	0,0048
24	Zn	0,1007
25	H_2O	1,43

The physical and chemical properties of shungite and zeolite have been sufficiently studied [8]. The density of shungite makes up 2,1–2,4 g/cm^3; the porosity – up to 5 %; the compressive strength – 1000–1200 kgf/cm^2; the conductivity coefficient – 1500 SI/m; the thermal conductivity coefficient – 3,8 W/m·K, the adsorption capacity – up to 20 m^2/g. The density of zeolite – 1,7–2,1 g/cm^3; the porosity – 50 %; the adsorption capacity is 5 m^2/g; an average pore size – 0,4–0,6 nm.

Shungites differ in composition of their mineral matrix (aluminosilicate, siliceous, carbonate), and the amount of carbon in schungite samples. The shungite minerals with silicate mineral basis are divided into the low-carbon (5 % C), medium-carbon (5–25 % C), and high-carbon schungites (25–80 % C) [9]. The sum of (C + Si) in shungites of the Zazhoginsky deposit (Karelia, Russian Federation) generally is varied within 83–88 % as shown in Figure 2. The molar ratios of SiO_2 and Al_2O_3 in the aluminosilicate framework of the zeolite comprise ~2–3 units.

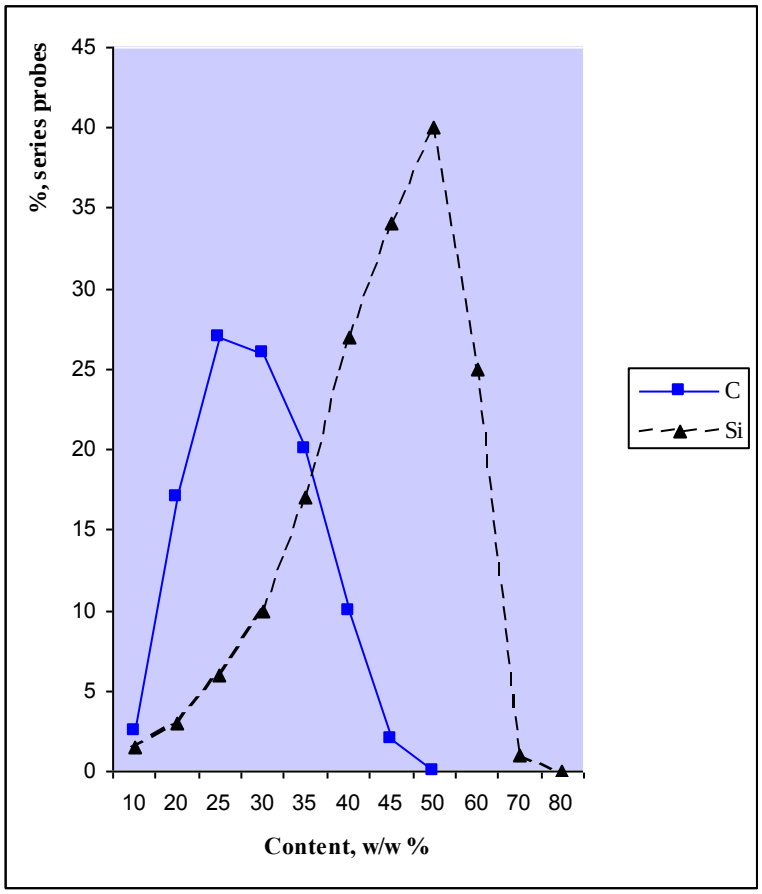

Figure 2. The distribution (%) of carbon (C) (solid line) and silicon (Si) (dotted line) in shungate samples from Zazhoginsky deposit (Karelia, Russian Federation) according to atomic emission spectrometry (AES)

The crystals of the crushed, fine ground shungite possess strong bipolar properties. This results in a high adhesion, and the ability of shungite to mix up with almost all organic and inorganic substances. Besides, shungite has a broad spectrum of bacterecidal properties; the mineral is the actively adsorptive against some bacterial cells, phages, and pathogenic saprophytes [10].

The unique properties of the mineral are defined by the nanostructure and composition of its constituent elements. The schungite carbon is equally distributed in the silicate framework of fine dispersed quartz crystals having the size of 1–10 μm [11, 12], as was confirmed by the studying of ultra-thin sections of shungite by transmission electron microscopy (TEM) in absorbed and backscattered electrons (Fig. 3).

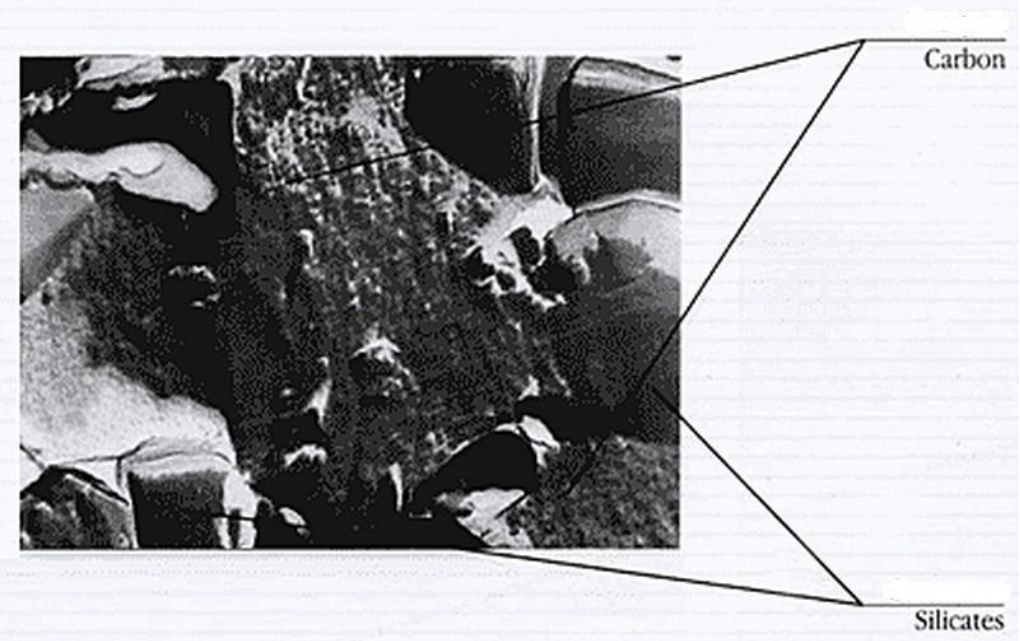

Figure 3. Structure of schungite rock obtained by the TEM method [11]. Scanning area 100×100 mm, resolution 0,5 nm, magnification 300000 times. The arrows show the silicate framework of fine dispersed quartz with the size 1–10 μm, and uniformly distributed carbon

The carbonaceous material of shungite is the product of a high degree of carbonization of hydrocarbons. Its elemental composition (%, w/w): C – 98,6–99,6; H – 0,15–0,5; (H + O) – 0,15–0,9 [13]. With virtually constant elemental composition of shungite, the carbonaceous matter is demonstrated the variability in its structure – both molecular and supramolecular, as well as surface, and porous structure. X-ray studies showed that the molecular structure of schungite carbon is represented by a solid uncristallized carbon, which components may have been in a state close as to the graphite and the carbon black and the glassy carbon as well, i.e. the maximally disordered [14]. The carbonaceous matter of shungite having a strongly marked structural anisotropy shows a significant increase in the diamagnetism at low temperatures that is a characteristic feature for fullerites [15].

The basis of the shungite carbon compose the hollow carbon fullerene-like multilayer spherical globules with a diameter of 10–30 nm, comprizing inclusive packages of smoothly curved carbon layers covering the nanopores (Fig. 4). The globule structure is stable relative to the shungite carbon phase transitions into other allotropic carbon forms. The fullerene-like globules (the content of fullerenes makes up ~0,001 %) may contain from a few dozen to a several hundred carbon atoms and may vary in shape and size [16].

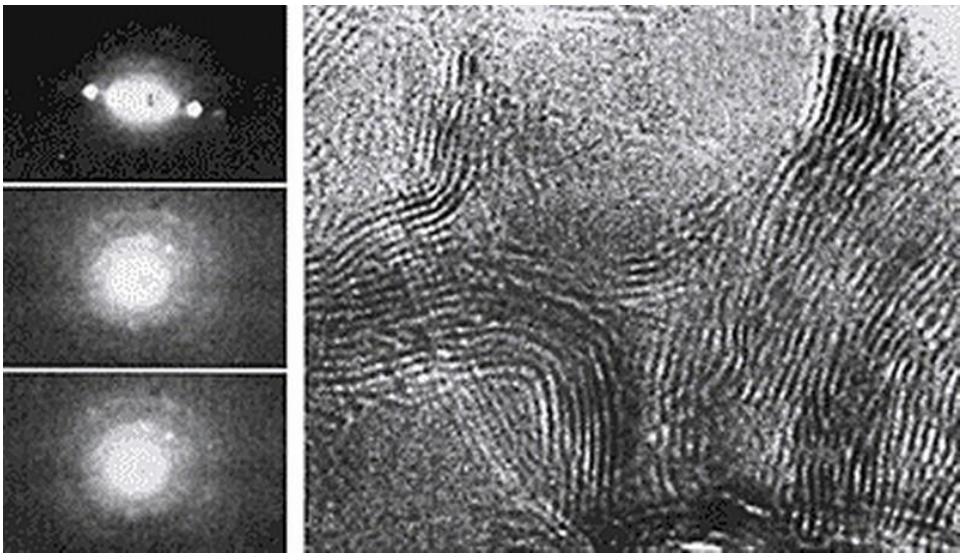

Figure 4. Electron diffraction of nanopattern of shungite carbon in the form of spherical multilayer fullerene globules with a diameter 10–30 nm, obtained by the TEM method [14] (the probe size 0,5–0,7 nm, the energy of the electron beam 100–200 kV, the beam radius 10 nm, the range of the goniometer rotation -27°...+27 °). On the left are shown fluoresent spherical fullerene-like globules, on the right – the multi-layered spherical fullerene-like globules with packets of carbon layers, recorded at a higher resolution

Moreover, the carbonaceous matter of shungite has structural anisotropy and shows a significant increase of diamagnetism at low temperatures characteristic to the crystals formed by fullerene molecules (fullerites) [17]. Fullerites are molecular crystals with a faced-centered cubic (FCC) lattice size of 1,42 nm, the number of nearest neighbors – 12 and the distance between them – 1 nm. The density of fullerite is 1,7 g/cm^3, which is slightly lower than the density and shungite (2,1–2,4 g/cm^3), and graphite (2,3 g/cm^3). Fullerene molecules may comprise 24, 28, 32, 36, 50, 60, 70, etc. carbon atoms (Fig. 5). Fullerenes with the number of carbon atoms n < 60 are unstable. Higher fullerenes containing more carbon atoms (n < 400) are produced in small quantities and often have rather difficult isomer composition [18]. The carbonaceous material of shungite in its composition contains fullerenes (C60, C70, C74, C76, C84, etc.), and fullerene-like structures, as separate and as well as related with minerals [19].

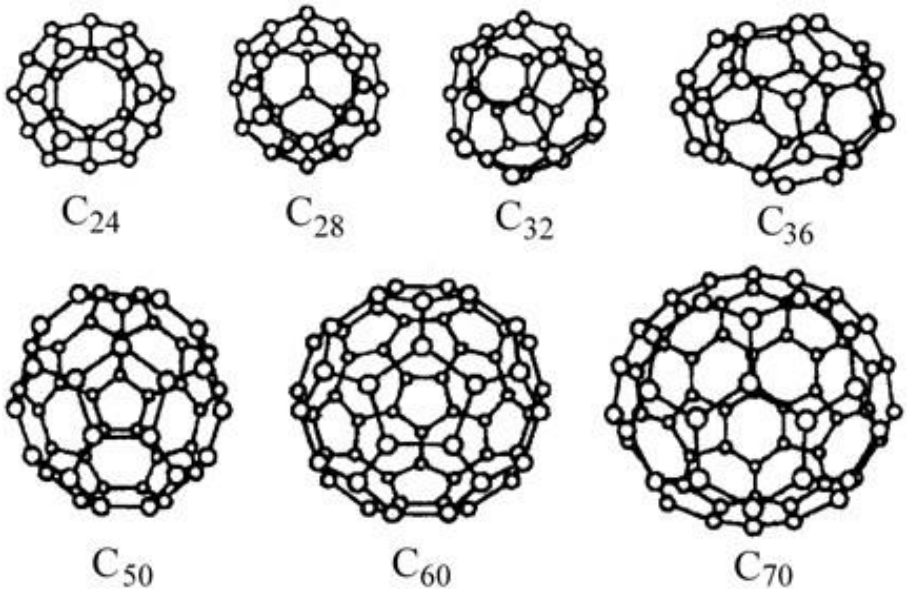

Figure 5. Varieties of fullerenes found in natural shungite with different numbers of carbon atoms: C24, C28, C32, C36, C50, C60, C70

Currently, the research is underway to modify the natural shungites to produce a mixed nanocarbon materials and increase the aggregate stability of the carbon nanoparticles in aqueous colloidal solutions of shungites and fullerenes [20]. It is also being discussed the idea of creating a drug carriers based on water-soluble endohedral fullerene compounds and natural fullerene material in which is placed inside one or more atoms of an element with radioactive isotopes. The conditions of synthesis of antiviral and anticancer drugs based on fullerenes, which introduction into the body allow a selective impact on the affected cancer cells, thus preventing their further reproduction. The prospects of development of the fullerene synthesis associated with the peculiarities of the chemical structure of fullerene molecules – the three dimensional analogues of aromatic structures and the presence of a large number of double conjugated bonds and reaction centers on a closed carbon sphere. Fullerenes having the high electronegativity, act in chemical reactions as a strong oxidizing agents. By allying to itself the radicals of different chemical nature, fullerenes can form a wide class of chemical compounds having different physico-chemical properties. At the present time it was synthesized about 3 thousand compounds based on fullerenes.

IR-studies of shungite

A convenient method to obtain information on the composition and the structure of a mineral is IR spectroscopy. IR spectra can usually be obtained with the amount of 0,5–3,0 mg of the sample, i.e. significantly less than required for NMR. In contrast to the NMR the measuring of IR-spectra is possible for solid compounds, which allows the study even insoluble solid substances.

By the method of IR-spectroscopy in the range of vibrations in the crystal mineral framework it is possible to obtain the information:

a) on the composition of the mineral and its components;

b) on the structure of the framework, particularly the lattice ratio type C/SiO_2 or SiO_2/Al_2O_3;

c) on the nature of the surface of the structural groups, which often serve as adsorption and catalytically active sites.

The wave absorption in the infrared region (400–4000 nm) is caused by the vibrational motion of the molecules associated with changes in bond lengths (stretching vibrations, v) or bond angles between the atoms (deformation vibrations, δ). The IR spectrum of the carbon containing organic compound ranges from 400–4000 cm^{-1} and allows identify these compounds. However, often the interpretation of natural carbon-containing minerals is difficult due to their multi-component composition and as the result numerous oscillations in samples. Furthermore, the number of absorption bands in the IR spectra may differ from the number of normal molecular vibrations due to the occurrence of additional bands: overtones, component frequencies, and overlapping lines due to the Fermi resonance.

The research of shungite with using the method of IR-spectroscopy revealed the presence at least seven main maxima in the IR-spectrum of shungite, detected at 2,90; 3,18; 3,32; 6,13; 7,14; 8,59; 9,21 μm (wave length, λ), or 3448; 3141; 3016; 1630; 1400; 1164 and 1086 cm^{-1} (wave number, k) corresponding to oscillations of various organic group types in shungite (Fig. 6).

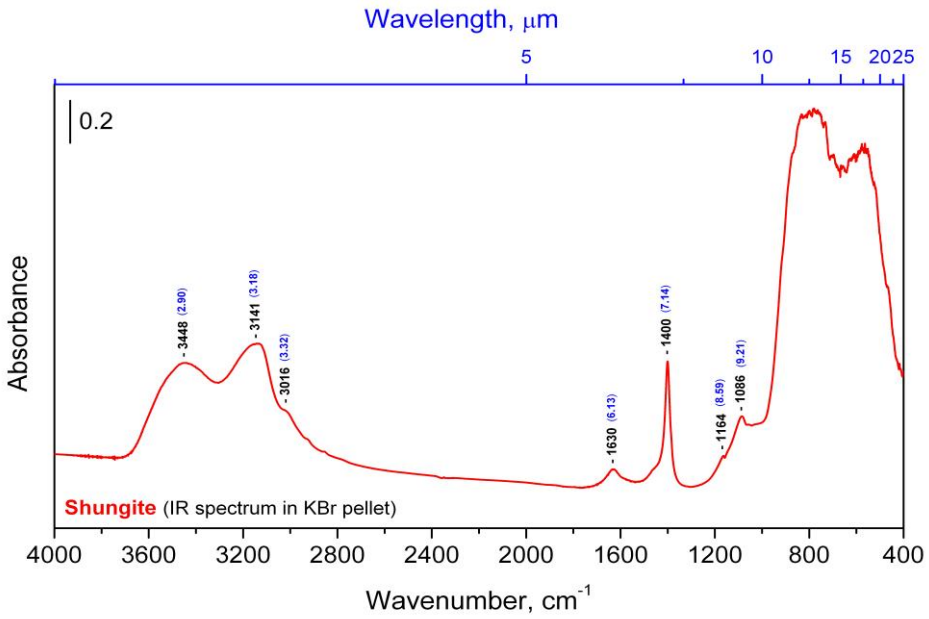

Figure 6. IR-spectrum of shungite in KBr pellet (the spectral range: average IR – 370–7800 cm^{-1}; visible – 2500–8000 cm^{-1}; the permission – 0,5 cm^{-1}; accuracy of wave number – 0,1 cm^{-1} on 2000 cm^{-1})

The average IR region is the most informative and marked as fundamental. In turn, this area is divided into the "fingerprint" region (700–1500 cm^{-1}) and the region of characteristic bands (1500–4000 cm^{-1}).

When interpreting the IR spectra of the organic samples the most informative is the region at 2500–1500 cm^{-1} and the region at 4000–2500 cm^{-1}. Analysis of the first of these allows determine the presence in the sample the unsaturated compounds: C=C, C≡C, C=O, C=N, C≡N, as well as the aromatic and heteroaromatic nucleus. The absorption bands in the region at 4000–2500 cm^{-1} can identify functional groups as O–H, N–H, S–H, as well as various types of carbon-hydrogen C_{sp3}–H, C_{sp2}–H, C_{sp}–H, (O=) C–H-bonds.

The IR spectra of organic compounds can be divided into three main areas (Table 4):

1) 4000–2500 cm^{-1} – a region of stretching vibrations of single bonds X–H: O–H, N–H, C–H, S–H;

2) 2500–1500 cm^{-1} – a region of stretching vibrations of multiple bonds X=Y, X≡Y: C=C, C=O, C=N, C≡C, C≡N;

3) 1500–500 cm^{-1} – a region of stretching vibrations of single bonds X–Y: C–C, C–N, C–O and deformation vibrations of single bonds X–H: C–H, O–H, N–H.

Table 4: Characteristic vibrational frequencies of organic compounds [13]

Groups and types of oscillations	The range of frequencies (cm^{-1}), the intensity of the absorption bands
Covalent C–H bond	
Alkanes C_{sp3}–H stretching, v deformational (I) deformational (II)	 2975–2860 (intensive) 1470–1430 (average) 1380–1370 (intensive)
O–CH_3 Stretching	 2820–2810 (intensive)
CH_3Hal (F, Cl, Br, I) stretching, v	 3058–3005 (intensive)

Alkenes C_{sp2}–H stretching, v (=CH_2) deformational, δ (–CH=CH_2) stretching, v (=CH–) deformational, δ (–CH=CH–) *trans-* *cis-*	 3095–3075 (average) 1420–1410 (intensive) 3040–3010 (average) 1310–1295 (average) 970–960 (intensive) ~690 (average)
Aromatic hydrocarbon $C_{arom.}$–H stretching, v deformational, δ	 ~3030 (intensive) 900–690 (intensive)
Aldehydes stretching, v (I) stretching, v (II)	 2900–2820 (not intensive) 2775–2700 (not intensive)
Alkynes C_{sp}–H stretching, v (≡C–H) deformational, δ (–C≡C–H)	 ~3300 (intensive) 680–610 (intensive)
Covalent bonds X–H	
O–H stretching, v deformational, δ	 3650–3590 (average, narrow) 1450–1250 (average, wide)
H-linked bond stretching, v: alcohols, phenols, carbohydrates, carboxylic acids	 3550–3200 (intensive, wide) 2700–2500 (wide)
N–H Primary amines and amides (–NH–) stretching, v (2 bands) deformational, δ (amid band II)	 3500–3300 (average) 1650–1590 (intensive-average)
Secondary amines and amides (–NH–) stretching, v (I band) deformational, δ (amide band II)	 3500–3300 (average) 1650–1550 (not intensive)
Amino acids stretching, v (NH_3^+) amino acid band I amino acid band II	 1660–1610 (not intensive) 1550–1485 (average)
Imines (+NH–) stretching, v (I band)	 3400–3300 (average)
S–H stretching, v	 2600–2550 (average)
P–H stretching, v	 2440–2350 (average, wide)
Si–H stretching, v	 2280–2080 (average)
Covalent bonds X–Y	
C_{sp3}–C_{sp3} stretching, v	 1250–1200 (intensive)
C–O stretching, v: primary alcohols secondary alcohols tertiary alcohols phenols	 1075–1000 (intensive) 1150–1075 (intensive) 1210–1100 (intensive) 1260–1180 (intensive)

Ethers	
di-alkyl (–CH_2–O–CH_2–)	1150–1060 (very intensive)
aromatic (Ar–O–Ar)	1270–1230 (very intensive)
C–N	
stretching, v:	
aliphatic amines	1220–1020 (average-not intensive)
primary aromatic amines	1340–1250 (intensive)
secondary aromatic amines	1350–1280 (intensive)
tertiary aromatic amines	1360–1310 (intensive)
aliphatic nitro compounds	920–830 (intensive)
aromatic nitro compounds	860–840 (intensive)
C–Hal	
stretching, v:	
C–F	1400–1000 (very intensive)
C–Cl	800–600 (intensive)
C–S	
stretching, v	710–570 (not intensive)
C–P	
stretching, v	800–700 (shifting)
C–O	
stretching, v	870–690 (shifting)
Double covalent bonds X=Y	
C=C	
stretching, v	
isolated double bond (C=C)	
alkenes	1670–1620 (shifting)
cumulated double bonds (C=C=C)	
allenes	~1950 (intensive)
	~1060 (average)
Conjugated double bonds	
(C=C–C=C or C=C–C=O)	
alkadienes and enones	1640–1600 (intensive)
benzene ring (multiple bands)	~1600 (shifting)
	~1580 (shifting)
	~1500 (shifting)
	~1450 (shifting)
C=O	
stretching, v	
saturated aldehydes, ketones, carboxylic acid esters	1750–1700 (intensive) 1755–1720 (intensive)
a-amino acids (COOH)	1600–1560 (intensive)
amino acids (COO^-)	1705–1660 (intensive)
unsaturated aldehydes and aromatic ketones	1700–1630 (intensive)
amides (amid band I)	
C=N	
stretching, v	1690–1630 (shifting)
C=S	
stretching, v	1200–1050 (intensive)
N=O	
stretching, v	
nitrites (–O–N=O) (2 bands)	1680–1610 (intensive)
nitroso (–C–N=O)	1600–1500 (intensive)
nitrosamines (–N–N=O)	1500–1430 (intensive)
C=S	
stretching, v	1200–1050 (intensive)

In the sub-region (700–1500 cm^{-1}) are located the absorption bands of the skeleton of the organic molecules comprising C–C-bond, C–O, C–N (for this region are not characteristic oscillations belonging to separate bonds). The nature of the IR-spectrum in this frequency range varies significantly with small differences in the spectra of the organic compounds, as each compound has its unique distinctive set of absorption bands. It can be used to discriminate between the molecules having the same functional group.

In the spectral range of 1500–4000 cm^{-1} are located all fluctuations of the basic functional groups. These groups act as if being isolated and independently of the rest of the molecule, as their absorption frequencies little change at transition from one compound to another. The characteristic may be the bands corresponding to both the stretching and bending vibrations.

Absorption in the region at 1400–1300 cm^{-1} and 700 cm^{-1} is due to deformation oscillations of CH_3- and CH_2-groups. The stretching vibrations of the terminal C=C bond correspond to the average intensity of the band at 1640 cm^{-1}.

The position band of CH_2-group at 800–700 cm^{-1} is dependent on the carbon chain length and is used to detect the organic compounds containing the polymethylene chain.

In the region of 3095–3010; 2975; 3040–3010 cm^{-1} are located stretching vibrations of C–H aromatic, heteroaromatic, small cycles, halogenated alkyl groups.

The main range of characteristic bands of organic compounds changes from 3100–3000 cm^{-1} for H–C-; N–H-; O–H-bonds; 3100–2800 cm^{-1} – for C–H; $-CH_3$-bonds; 3040–3010 cm^{-1} – for =CH-bonds; 1750–1700 cm^{-1} – for C=O bonds; 1690-1630 cm^{-1} – for C=N-bonds; 1670–1620 cm^{-1} – for C=C-bonds; 1420–1410 cm^{-1} – for CH_2=CH-bonds; 1310-1295 cm^{-1} – for –CH=CH-bonds; 1250–1200 cm^{-1} – for C_{sp3}–C_{sp3}-bonds; 1260–1000 cm^{-1} for C–O-bonds; 1220–1020 cm^{-1} – for C–N-bonds; 1400–1300 cm^{-1} – for CH_2-bonds; 1640–1600 cm^{-1} – for C=C–C=C or C=C–C=O-bonds; 1060–1950 cm^{-1} for conjugated double C=C=C-bonds (Table 3).

Absorption in the region at 3000–2800 cm^{-1} appears as complex band absorption. The position of bands in this area is preserved in all types of aliphatic hydrocarbons. The intensity of the bands depends on the number of CH_2- and CH_3-groups in the molecule. The accumulation of CH_2-groups increases the intensity of the absorption band of 3000–2800 cm^{-1}, whereas the intensity of the band of the CH_3–group changes little. This property is used for quantitative analysis of hydrocarbons. Thus, the carbonaceous composition of shungite is complex; this mineral contains in its composition many functional groups of organic compounds with different types of bonds, which is due to its complex organic composition.

Evaluation of the mathematical model of interaction of shungite and zeolite with water

Other method for obtaining the information about the average energy of hydrogen bonds in an aqueous sample is measuring the spectrum of the water state. It was established experimentally that at evaporation of water droplet the contact angle θ decreases discretely to zero, whereas the diameter of the droplet changes insignificantly [21]. By measuring this angle within a regular time intervals a functional dependence f(θ) can be determined, which is designated by the spectrum of the water state (SWS) [22–24]. For practical purposes by registering the SWS it is possible to obtain information about the averaged energy of hydrogen bonds in an aqueous sample. For this purpose the model of W. Luck is used, which consider water as an associated liquid, consisted of O–H...O–H groups [25]. The major part of these groups is designated by the energy of hydrogen bonds (-*E*), while the others are free (*E* = 0). The energy distribution function *f(E)* is measured in electron-volts (eV^{-1}) and may be varied under the influence of various external factors on water as temperature and pressure.

For calculation of the function *f(E)* the experimental dependence between the water surface tension measured by the wetting angle (*θ*) and the energy of hydrogen bonds (*E*) in an aqueous sample is used:

$$f(E) = \frac{14{,}33\, f(\theta)}{[1-(1+bE)^2]^2},$$

where b = 14,33 eV^{-1}; $\theta = arcos(-1 - b\ E)$

The energy of hydrogen bonds (E) measured in electron-volts (eV) is designated as the spectrum of energy distribution. This spectrum is characterized by non-equilibrium process of water droplets evaporation, thus the term "non-equilibrium energy spectrum of water" (NES) is applied.

The difference $\Delta f(E) = f(E_{\text{samples of water}}) - f(E_{\text{control sample of water}})$

– is designated the "differential non-equilibrium energy spectrum of water" (DNES).

The DNES is a measure of changes in the structure of water as a result of external factors, because the energy of hydrogen bonds in water samples differ due to the different number of hydrogen bonds in water samples, which may result from the fact that different waters have different structures and composition and various intermolecular interactions – the various associative elements etc. The redistribution of H_2O molecules in water samples according to the energy is a statistical process of dynamics.

It was studied the distribution of local extremums in water solutions of of shungite and zeolite regarding the energies of hydrogen bonds. The average energy ($\Delta E_{H...O}$) of hydrogen H…O-bonds among individual H_2O molecules was calculated for the water solutions of of shungite and zeolite by NES- and DNES-methods. The research with the NES method of water drops, received after their being exposed for 3 days with shungite and zeolite in deionized water, may also give valuable information on the possible number of hydrogen H…O-bonds as a percent (%) of individual H_2O molecules with different values of distribution of energies of hydrogen bonds (Table 5). These distributions are basically connected with the re-structuring of H_2O molecules with the same energies.

Table 5: Characteristics of spectra of water after 3 days infusion with shungite and zeolite, obtained by NES-method

-E(eV) x-axis	Shungite, % [$(-E_{value})/(-E_{total\ value})$]	Zeolite, % [$(-E_{value})/(-E_{total\ value})$]	-E(eV) x-axis	Shungite, % [$(-E_{value})/(-E_{value})$]	Zeolite, % [$(-E_{value})/(-E_{total\ value})$]
0,0937	2,85	6,3	0,1187	0	12,4
0,0962	8,8	6,3	0,1212	5,9	6,3
0,0987	5,9	0	0,1237	0	0
0,1012	11,8	12,4	0,1262	0	0
0,1037	11,8	6,3	0,1287	0	18,7
0,1062	0	6,3	0,1312	8,8	6,3
0,1087	0	0	0,1337	2,85	0
0,1112	5,9	0	0,1362	0	0
0,1137	11,8	0	0,1387	11,8	2,4
0,1162	11,8	6,3	–	–	–

The distribution [%, $(-E_{value})/(-E_{total\ value}$] of H_2O molecules in water solution of shungite/zeolite according to energies of hydrogen bonds and local extremums in NES and DNES spectra of water solutions of of shungite and zeolite is shown in Figure 6 and Table 6. The average energy ($\Delta E_{H...O}$) of hydrogen H…O-bonds among individual molecules H_2O after the treatment of shungite and zeolite with water was measured to be at -0,1137 eV for shungite and -0,1174 eV for zeolite. The result for the control sample (deionized water) was -0,1162 eV. The results obtained with the NES method were recalculated with the DNES method. Thus, the result for shungite measured with the DNES method was +0,0025±0,0011 eV and -1,2±0,0011 eV for zeolite. This difference may indicate on the different mechanisms of interaction of these minerals with water, but also may has been the result of the different composition and the structure of these two minerals, resulting in different behavior while the interaction with water.

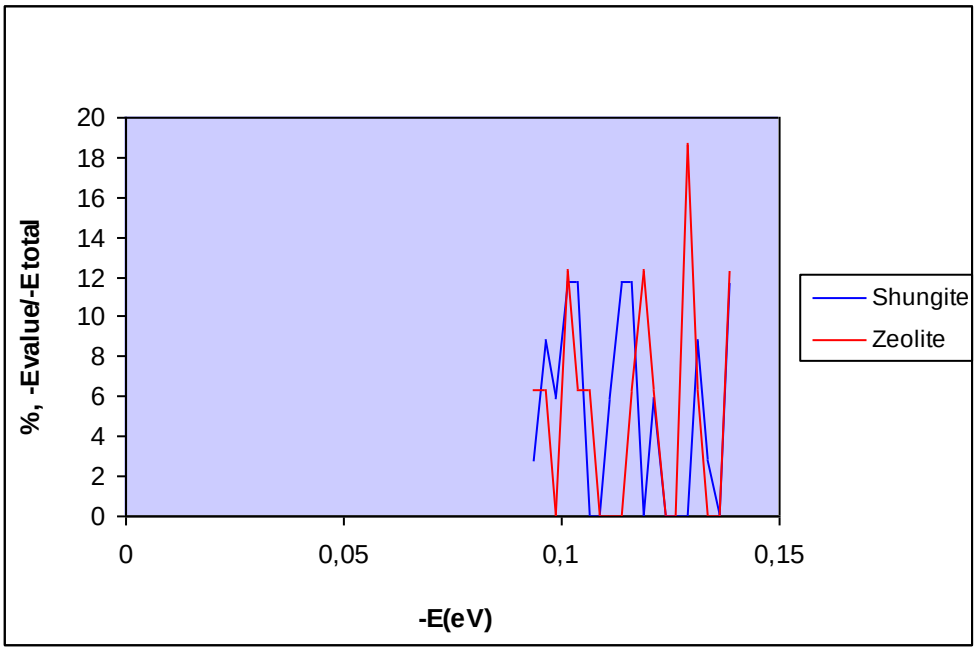

Figure 6. The distribution [%, ($-E_{value}$)/($-E_{total\ value}$] of water molecules in water solution of shungite/zeolite according to energies of hydrogen bonds ($-E_{value}$) to a total result of hydrogen bonds energy

Table 6: Distribution of energies of hydrogen bonds and the local extremums in NES and DNES spectra of water solutions of shungite and zeolite

-E(eV) x-axis	NES Shungite	NES Zeolite y-axis (eV^{-1})	NES Control sample y-axis (eV^{-1})	DNES Shungite y-axis (eV^{-1})	DNES Zeolite y-axis (eV^{-1})	-E(eV) x-axis	NES Shungite y-axis (eV^{-1})	NES Zeolite y-axis (eV^{-1})	NES Control Sample y-axis (eV^{-1})	DNES Shungite y-axis (eV^{-1})	DNES Zeolite y-axis (eV^{-1})
0,0937	11,8	25,0	0	11,8	25,0	0,1187	0	50,0	30,8	-30,8	19,8
0,0962	35,3	25,0	30,8	4,5	-5,8	0,1212	23,5	25,0	30,8	7,3	5,8
0,0987	23,5	0	0	23,5	0	0,1237	0	0	0	0	0
0,1012	47,1	50,0	0	47,1	50,0	0,1262	0	0	30,8	-30,8	-30,8
0,1037	47,1	25,0	30,8	16,3	-5,8	0,1287	0	75,0	0	0	75,0
0,1062	0	25,0	0	0	25,0	0,1312	35,3	25,0	0	35,3	25,0
0,1087	0	0	76,9	-76,9	-76,9	0,1337	11,8	0	30,8	-19,0	-30,8
0,1112	23,5	0	15,4	8,1	-15,4	0,1362	0	0	15,0	-15,0	-15,0
0,1137	47,1	0	30,8	16,3	-30,8	0,1387	47,1	50,0	15,0	32,1	35,0
0,1162	47,1	25,0	61,5	-14,4	-36,5	–	–	–	–	–	–

The results also suggest the restructuring of the energy values among the individual H_2O molecules with a statistically reliable increase of local maximums in DNES-spectra. For the value -0,1387 eV there was a local maximum with positive values for shungite and zeolite. In this regard it should be noted that A. Antonov early demonstrated that in the aqueous suspension of tumor cells there was detected a decrease of local maximums; DNES-spectra of aqueous solution containing Ca^{2+} have a local minimum of energy at -0,1 eV and a local maximum at -0,11 eV. The interesting fact is that due to the present of calcium in shungite, the aqueous solution of shungite has a local minimum of energy at -0,0987 eV and a local maximum at -0,1137 eV that closely corresponds with the DNES-spectrum of aqueous solution containing Ca^{2+}. Thus, by the analyzing the NES- and DNES-spectra of aqueous solutions of shungite and zeolite in water it is possible to evaluate the base of the mathematical model of interaction of these minerals with water, judging by the

structural properties, the energies of of hydrogen H…O-bonds and the distribution the individual H_2O molecules in samples with different values of energies.

Table 7 shows the local extremums in spectra of different samples of mountain water, as well as ions of Ca^{2+}, Na^{+}, Mg^{2+}, Fe^{2+}, SO_4^{2-} and pH values. For all these types of water is applied a new parameter in Table 6 – the local extremum, measured at -0,1362…-0,1387 eV. Its value in the NES-spectrum is measured as the function of distribution of individual H_2O molecules in water samples according to energy *f(E)* of hydrogen bonds. The function of distribution of individual H_2O molecules according to energy *f(E)* of hydrogen bonds for tap water from Teteven (Bulgaria) is measured up at 23,8±1,2 eV^{-1}.

Table 7: The composition of mountain water sources from Teteven (Bulgaria), their pH values and local extremums in spectra after exposition with shungite

Water sources	Ca^{2+}	Na^{+}	Mg^{2+}	Fe^{2+}	SO_4^{2-}	pH	Local extremum* at (-0,1362…-0,1387 eV) (1)	Local extremum* with shungite (-0,1362…-0,1387 eV) (2)	Difference between (2) and (1)
	mg/dm^3 norm (<150)	mg/dm^3 norm (<200)	mg/dm^3 norm (<80)	mg/dm^3 norm (<200)	mg/dm^3 norm (<250)	norm (6,5–9,5)	eV^{-1} norm (>24,1)	eV^{-1} norm (>24,1)	eV^{-1} norm (>24,1)
1. Deionized water (control)	–	–	–	–	–	–	15,4 ±0,8	47,1 ±2,8	31,7 ±1,6
2. Klindiovo	89,9 ±9,0	4,1 ±0,4	6,98 ±0,7	40,2 ±4,0	17,7 ±1,8	8,0 ±0,1	44,4 ±2,2	63,2 ±3,2	18,6 ±0,9
3. Gorna cheshma	103,6 ±10,4	4,2 ±0,4	15,5 ±1,6	9,6 ±0,96	89,9 ±9,0	7,3 ±0,1	51,6 ±2,6	80,0 ±4,0	28,4 ±1,4
4. Dolna cheshma	94,4 ±0,94	2,5 ±0,3	12,10 ±1,21	9,0 ±0,9	15,99 ±1,6	7,9 ±0,1	34,2 ±1,7	51,6 ±2,6	17,4 ±0,9
5. Sonda	113,6 ±11,4	7,3 ±0,7	15,99 ±1,60	5,00 ±0,5	57,2 ±5,7	7,3 ±0,1	54,4 ±2,7	70,6 ±3,5	16,2 ±0,8
6. Ignatov izvor	40,44 ±4,04	0,62 ±0,12	2,46 ±0,25	13,0 ±1,4	17,9 ±1,8	6,82 ±0,1	48,0 ±2,4	85,7 ±4,3	37,7 ±1,9
7. Gechovoto	66,0 ±6,0	1,46 ±0,15	2,1 ±0,2	11,4 ±1,1	15,9 ±1,6	7,94 ±0,1	41,7 ±2,1	84,2 ±4,2	42,5 ±2,1

*Notes: The function of distribution of individual H_2O molecules according to energy *f(E)* of hydrogen bonds for tap water in Teteven (Bulgaria) is 23,8±1,2 eV^{-1}; results refer to the influence of shungite on different sources of mountain water according to energy *f(E)* of hydrogen bonds.

We have obtained new data for the influence of shungite on NES- and DNES-spectra of different mountain water sources and characteristics of spectra (Table 7). The peculiarities consist in the values of the local extremum measured at -0,1362…-0,1387 eV. It was detected the tendency of the increasing of local extremums in aqueous solution of shungite in water regarding the same mountain water samples as regard to the control sample. The distribution of local extremums detected at -0,1362…-0,1387 eV has an inversely character dependent for the ion content in water for the difference at -0,1362…-0,1387 eV of the shungite solution in mountain water and the same water as a control sample. These results suggest about the different mechanisms of interactions of these minerals with water with a statistically reliable increase of local maximums in DNES-spectra. The data obtained are very promising and further need to be scrutinized seriously. The research will be continued in future with new experiments.

Conclusion

The fullerene-containing natural mineral shungite and microporous crystalline aluminosilicate mineral zeolite have a complex multicomponent composition. The efficiency of using and studying these two natural minerals is stipulated by the high range of valuable properties (absorption, catalytic, antioxidant, regenerative), high environmental safety and relatively low cost of filters based on shungite and zeolite as well as existence of the extensive domestic raw material

base of shungite and zeolite deposits. All these factors contribute to the further studies. As the result of our studies the base of the mathematical model describing the interaction of these two minerals with water was established. It allows understand better, how these minerals interact with H_2O molecules in water solutions in order to explain the physical-chemical and adsorption properties of these minerals.

Aknowlegements

The authors wish to thank Engineer Assen Toshev (Sofia, Bulgaria) for his help in drawing the diagrams.

References:

1. Khavari-Khorasani G. The nature of carbonaceous matter in the Karelian shungite / G. Khavari-Khorasani, D.G. Murchison // *Chem. Geol.* 1979. V. 26. P. 165–82.

2. Mosin O.V. The structure and composition of natural carbonaceous fullerene containing mineral shungite / O.V. Mosin, I. Ignatov // *International Journal of Advanced Scientific and Technical Research*. 2013. V. 6, № 11–12. P. 9–21.

3. Gorshteyn A.E. Adsorption properties of shungites / A.E. Gorshteyn, N.Y. Baron, M.L. Syrkina // *Izv. Vysshykh Uchebn. Zaved. Khimia i Khim. Technol.* 1979. V. 22, № 6. P. 711–715 [in Russian].

4. Cascarini de Torre L.E. Characterization of shungite by physical adsorption of gases / L.E. Cascarini de Torre, A.E. Fertitta, E.S. Flores, J.L. Llanos, E.J. Bottani // *J. Argent. Chem. Soc.* 2004. V. 92, № 4–6. P. 51–58.

5. Podchaynov S.F. Mineral zeolite – a multiplier of useful properties shungite. Shungites and human safety, in *Proceedings of the First All-Russian scientific-practical conference* (3–5 October 2006) / Ed. J.K Kalinin. – Petrozavodsk: Karelian Research Centre of Russian Academy of Sciences. 2007. P. 6–74 [in Russian].

6. Volkova I.B. / I.B. Volkova, M.V. Bogdanov // Petrology and genesis of the Karelian shungite-high rank coal. *Int. J. Coal Geol.* 1986. V. 6. P. 369–79.

7. Panayotova M. Kinetics of heavy metal ions removal by use of natural zeolite / M. Panayotova, B. Velikov // *Journal of Environmental Science and Health*. 2002. V. 37, № 2. P. 139–147.

8. Parfen'eva L.S. Electrical conductivity of shungite carbon / L.S. Parfen'eva // *Solid State Physics*. 1994. V. 36, № 1. P. 234–236.

9. Kasatochkin V.I. Submikroporous structure of shungites / V.I. Kasatochkin, V.M. Elizen, V.M. Melnichenko, I.M. Yurkovsky, V.S. Samoilov // *Solid Fuel Chemistry*. 1978. № 3. P. 17–21.

10. Khadartsev A.A. Shungites in medical technologies / A.A. Khadartsev, I.S. Tuktamyshev // *Vestnik Novih Medicinskih Technologii*. 2002. V. 9, № 2. P. 83–86 [in Russian].

11. Kovalevski V.V. Structure of shungite carbon / V.V. Kovalevski // *Natural Graphitization Chemistry*. 1994. V. 39. P. 28–32.

12. Mosin O.V. Composition and structural properties of fullerene analogous mineral shungate / O.V. Mosin, I. Ignatov I // *Journal of Nano and Microsyctem Technique*. 2013. V. 1. P. 32–40 [in Russian].

13. Golubev E.A. *Local supramolecular structures shungite carbon* / E.A. Golubev // in Proceedings of the Int. Symp. "Carbon-formation in geological history". – Petrozavodsk: Publishing House of the Karelian Research Center, Russian Academy of Sciences. 2000. P. 106–110 [in Russian].

14. Kovalevski V.V. Comparison of carbon in shungite rocks to other natural carbons: an X-ray and TEM study / V.V. Kovalevski, P.R. Buseckb, J.M. Cowley // *Carbon*. 2001. V. 39. P. 243–256.

15. Jushkin N.P. Globular supramolecular structure shungite: data scanning tunneling microscopy / N.P. Jushkin // *Reports. Acad. Science USSR*. 1994. V. 337, № 6. P. 800–803 [in Russian].

16. Reznikov V.A. Shungite amorphous carbon – the natural environment of fullerene / V.A. Reznikov, Y.S. Polehovsky // *Technical Physics Letters*. 2000. V. 26, № 15. P. 689–693.

17. Kalinin Yu.K. The structure of the shungite carbon and possibility of the presence of fullerenes / Yu.K. Kalinin // *Solid State Chemistry*. 2002. № 1. P. 20–28.

18. Mosin O.V. The Composition and structural properties of fullerene natural mineral shungite / O.V. Mosin, I. Ignatov // *Nanoengineering*. 2012. V. 18, № 12. P. 17–24 [in Russian].

19. Pleshakov V. Computer models of icosahedral carbon nanostructures (shungite) / V. Pleshakov // *J. Appl. Cryst*. 2014. V. 47. P. 539–543.

20. Ignatov I. The structure and composition of carbonaceous fullerene containing mineral shungite and microporos crystalline alumosilicate mineral zeolite / I. Ignatov, O.V. Mosin // *Nanotechnology Research and Practice*. 2014. V.1, № 1. P. 30–42.

21. Antonov A. *Research of the nonequilibrium processes in the area in allocated systems* / A. Antonov. Diss. thesis doctor of physical sciences. – Sofia: Blagoevgrad. 2005. P. 1–255.

22. Ignatov I. Structural mathematical models describing water clusters / I. Ignatov, O.V. Mosin // *Journal of Mathematical Theory and Modeling*. 2013. V. 3, № 11. P. 72–87.

23. Ignatov I. *Energy Biomedicine* / Ed. I. Ignatov. – Sofia: Gea-Libris. 2005. P. 1–88.

24. Ignatov I. Water in human body is informational bearer about longevity / I. Ignatov // in *Conference on the Physics, Chemistry and Biology of Water*. – Vermont Photonics. USA, 2012. P. 137.

25. Luck W. Infared investigation of water structure in desalination membranes / W. Luck, D. Schiöberg, S. Ulrich // *J. Chem. Soc. Faraday Trans*. 1980. V. 2, № 76. P. 136–147.

УДК 541.64:574.24:553.08

Методы неравновесного энергетического спектра и дифференциального неравновесного энергетического спектра в изучении взаимодействия углеродсодержащего минерала шунгита и алюмосиликатного минерала цеолита с водой

[1] Игнат Игнатов
[2] Олег Викторович Мосин

[1] Научно-исследовательский центр медицинской биофизики (РИЦ МБ), Болгария
Профессор, доктор наук Европейской академии естественных наук (ФРГ), директор НИЦ МБ.
1111, София, ул. Н. Коперника, 32/6
E-mail: mbioph@dir.bg
[2] Московский государственный университет прикладной биотехнологии, Российская Федерация
Старший научный сотрудник кафедры биотехнологии, канд. хим. наук.
103316, Москва, ул. Талалихина, 33
E-mail: mosin-oleg@yandex.ru

Аннотация. Построена математическая модель взаимодействия с водой аморфного, некристаллизирующегося, фуллереноподобного углеродсодержащего минерала шунгита (Зажогинское месторождение, Карелия, РФ) и микропористого кристаллического алюмосиликатного минерала цеолита (Мост, Болгария). Приведены данные о наноструктуре, а также о составе и химико-физические свойства этих минералов, полученные с помощью элементного анализа, сканирующей электронной микроскопии (СЭМ) и ИК-спектроскопии. Для построения математической модели взаимодействия этих минералов с водой использовали методы неравновесного энергетического спектра (НЭС) и дифференциально-неравновесного энергетического спектра (ДНЭС). Измерены величины средней энергии ($\Delta E_{H...O}$) водородных H...O-связей между молекулами H_2O после обработки шунгита и цеолита водой, составляющие -0,1137 эВ для шунгита и -0,1174 эВ для цеолита. Расчет $\Delta E_{H...O}$ для шунгита с использованием ДНЭС-метода составляет +0,0025±0,0011 эВ, а для цеолита -1,2±0,0011 эВ. Показана закономерность изменения энергии водородных связей между молекулами H_2O при обработке воды шунгитом и цеолитом со статистическим повышением локальных максимумов в ДНЭС-спектрах воды.

Ключевые слова: шунгит, цеолит, наноструктура, фуллерены, ИК, НЭС, ДНЭС

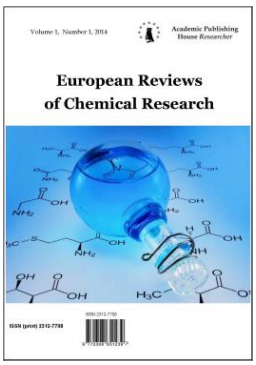

Published in the Russian Federation
European Reviews of Chemical Research
Has been issued since 2014.
ISSN: 2312-7708
E-ISSN: 2413-7243
Vol. 6, Is. 4, pp. 211-231, 2015

DOI: 10.13187/ercr.2015.6.211
www.ejournal14.com

UDC 579.871.08

Studying the Biosynthesis of ^{2}H-labeled purine Ribonucleoside Inosine by a Chemoheterotrophic Bacterium *Bacillus subtilis B-3157*

[1*] Oleg Mosin
[2] Ignat Ignatov

[1] Moscow State University of Applied Biotechnology, Russian Federation
Senior research Fellow of Biotechnology Department, Ph. D. (Chemistry)
103316, Moscow, Talalihina ulitza, 33
*E-mail: mosin-oleg@yandex.ru
[2] The Scientific Research Center of Medical Biophysics (SRC MB), Bulgaria
Professor, D. Sc., director of SRC MB
1111, Sofia, N. Kopernik street, 32
E-mail: mbioph@dir.bg

Abstract

We studied the biosynthesis of ^{2}H-labeled purine ribonucleoside inosine excreted into liquid microbial culture (LC) by Gram-positive chemoheterotrophic bacterium *Bacillus subtilis B-3157* while growing of this bacterium on heavy water (HW) medium with 2% (v/v) hydrolysate of deuterated biomass of the methylotrophic bacterium *Brevibacterium methylicum B-5662* as a source of ^{2}H-labeled growth substrates. Isolation of ^{2}H-labeled inosine from the LC was performed by adsorption/desorption on activated carbon with following extraction by 0,3 M ammonium–formate buffer (pH = 8,9), crystallization in 80% (v/v) EtOH, and ion exchange chromatography (IEC) on a column with AG50WX 4 cation exchange resin equilibrated with 0,3 M ammonium–formate buffer and 0,045 M NH_4Cl. The investigation of deuterium incorporation into the inosine molecule by FAB method demonstrated the incorporation of 5 deuterium atoms into the molecule (the total level of deuterium enrichment – 65,5 atom% ^{2}H) with 3 deuterium atoms included into the ribose and 2 deuterium atoms – into the hypoxanthine residue of the molecule. Three non-exchangeable deuterium atoms were incorporated into the ribose residue owing to reactions of enzymatic izomerization of glucose in ^2H_2O-medium. These non-exchangeable deuterium atoms in the ribose residue were originated from glycolysis, associated with the Embden-Meyerhof pathway, while two other deuterium atoms at C2,C8-positions in the hypoxanthine residue were synthesized from [^{2}H]amino acids that originated from the deuterated hydrolysate of the methylotrophic bacterium *Brevibacterium methylicum B-5662*. However, the effect of auxotrophy of this strain in tyrosine, histidine, adenine and uracilб presupposes the branched metabolic pathways, different those indicated above.

Keywords: ^{2}H-labeled inosine, biosynthesis, metabolism, heavy water, *Bacillus subtilis*, FAB mass-spectrometry.

Introduction

Natural nucleosides labeled with deuterium (^2H) are of considerable scientific and practical interest for various biochemical and diagnostic purposes [1], structural-functional studies [2], and research into cell metabolism [3]. Their usage is determined by the absence of radiation danger and the possibility of localizing the deuterium label in a molecule by ^1H-NMR [4], IR spectroscopy [5] and mass spectrometry [6] methods. The latter seems more preferable due to high sensitivity of the method and possibility to study the distribution of deuterium label *de novo*. The recent advance in technical and computing capabilities of these analytical methods has allowed a considerable increase the efficiency of carrying out biological studies with ^2H-labeled molecules *de novo*, as well as to carry out the analysis of the structure and function of nucleosides and their analogs at the molecular level [7]. In particular, ^2H-labeled ribonucleosides and their analogs are used in template-directed syntheses of deuterated RNA macromolecules for studying their spatial structure and conformational changes [8]. Perdeuteration and selective deuteration techniquemay be useful approaches for simplification of NMR spectra and for other structural studies of large biomolecules. Driven by the progress in multinuclear multidimensional NMR spectroscopy, deuteration of nucleic acids has especially found wide applications in the NMR studies of these macromolecules in solution. Deuterated ribonucleosides may be of further interest for NMR spectroscopy studies. Another usage of these deuterated molecules has been in atom transfer and kinetic isotope effect experiments.

An important factor in studies with ^2H-labeled nucleosides and their analogs is their availability. ^2H-labeled nucleosides can be synthesized with using chemical, enzymatic, and microbiological methods [9, 10]. Chemical synthesis is frequently multistage; requires expensive reagents and ^2H-labeled substrates, and eventually results to a racemic mixture of D- and L-enantiomers, requiring special methods for their separation [11]. Finer chemical synthesis of [^2H]nucleosides combines both chemical and enzymatic approaches [12].

Microbiology proposes an alternative method for synthesis of [^2H]nucleosides, applicable for various scientific and applied purposes; the main characteristics of the method are high outputs of final products, efficient deuterium incorporation into synthesized molecules, and preservation of the natural L-configuration of ^2H-labeled molecules [13]. A traditional approach for biosynthesis of ^2H-labeled natural compounds consists in growing of strains-producers on growth media containing maximal concentrations of ^2H_2O and ^2H-labeled substrates [14]. However, the main obstacle seriously implementing this method is a deficiency in ^2H-labeled growth substrates with high deuterium content. First and foremost, this stems from a limited availability and high costs of highly purified deuterium itself, isolated from natural sources. The natural abundance of deuterium makes up 0,015 atom%; however, despite low deuterium content in specimens, recently developed methods for its enrichment and purification allow to produce ^2H-labeled substrates with high isotopic purity.

Starting from first experiments on the growth of biological objects in heavy water, the approach involving hydrolysates of deuterated bacterial and micro algal biomass as growth substrates for growth of other bacterial strains-producers have been developed in this country [15]. However, these experiments discovered a bacteriostatic effect of ^2H_2O consisted in inhibition of vitally important cell functions in ^2H_2O; this effect on micro algal cells is caused by 70% (v/v) ^2H_2O and on protozoan and bacterial cells – 80–90% (v/v) ^2H_2O [16]. Attempts to use biological organisms of various taxonomic species, including bacteria, micro algae, and yeasts [17] for growth in ^2H_2O have not been widely used because of complexity of biosynthesis, consisted in need of complex growth media, applying intricate technological schemes, etc. That is why a number of applied items regarding the biosynthesis of natural ^2H-labeled compounds in ^2H_2O remain to be unstudied.

More promising seem the technological schemes involving as a source of ^2H-labeled growth substrates the biomass of methylotrophic bacteria, assimilating methanol *via* the ribulose-5-monophosphate (RMP) and serine pathways of carbon assimilation [18]. The assimilation rate of methylotrophic biomass by prokaryotic and eukaryotic cells makes up 85–98% (w/w), and their productivity calculated on the level of methanol bioconversion into cell components reaches 50–60% (w/w) [19]. As we have earlier reported, methylotrophic bacteria are convenient objects capable to grow on minimal salt media containing 2–4% (v/v) [^2H]methanol, whereon other

bacteria are unable to reproduce, and may easily be adapted to maximal ^2H_2O concentrations, that is the most important for the biosynthesis of ^2H-labeled natural compounds [20].

The aim of this research was studying the biosynthesis of ^2H-labeled inosine by a mutant strain of a Gram-positive chemoheterotrophic bacterium *Bacillus subtilis B-3157*.

Material and methods

Bacterial strain

The object of the research was a strain of inosine producer, spore-forming aerobic Gram-positive chemoheterotrophic bacterium *B. subtilis B-3157*, polyauxotrophic for histidine, tyrosine, adenine, and uracil (demand, 10 mg/l), obtained from Institute of Genetics and Selection of Industrial Microorganisms (Russia). The initial strain was adapted to deuterium by plating individual colonies onto 2% (w/v) agarose with stepwise increasing gradient of ^2H_2O concentration and subsequent selection of individual cell colonies stable to the action of ^2H_2O.

Chemicals

Growth media were prepared using ^2H_2O (99,9 atom% ^2H), ^2HCl (95,5 atom% ^2H), and [^2H]methanol (97,5 atom% ^2H), purchased from JSC "Izotop" (St. Petersburg, Russia). Inorganic salts, D- and L-glucose ("Reanal", Hungary) were preliminary crystallized in ^2H_2O. ^2H_2O was distilled over $KMnO_4$ with subsequent control of the isotope purity by ^1H-NMR spectroscopy on a Brucker WM-250 ("Brucker Daltonics" Germany) with a working frequency 70 MHz (internal standard – Me_4Si). According to ^1H-NMR, the level of isotopic purity of the growth medium was by 8–10 atom% lower than the isotope purity of the initial ^2H_2O.

Biosynthesis of [^2H]inosine

Biosynthetic [^2H]inosine was produced with an output 3,9 g/l in heavy water (HW) medium (89–90 atom% ^2H) using 2% (w/v) hydrolysate of deuterated biomass of the methanol assimilating strain of the facultative Gram-positive methylotrophic bacterium *Brevibacterium methylicum B-5662* as a source of ^2H-labeled growth substrates. The strain was obtained by multistage adaptation on a solid (2% (w/v) agarose) minimal salt M9 medium, containing 3 g/l KH_2PO_4, 6 g/l Na_2HPO_4, 0,5 g/l NaCl, 1 g/l NH_4Cl and 2% (v/v) [^2H]methanol with a stepwise increasing gradient of ^2H_2O concentration (0; 24,5; 73,5, and 98% (v/v) ^2H_2O). Raw methylotrophic biomass (output, 200 g/l) was suspended in 100 ml of 0,5 N ^2HCl (in ^2H_2O) and autoclaved for 30–40 min at 0,8 atm. The suspension was neutralized with 0,2 N KOH (in ^2H_2O) to pH = 7,0 and used as a source of growth substrates while growing the inosine producer strain. For this purpose, an inoculum (5–6 % (w/v)) was added into HW medium with 99,8 atom% ^2H_2O containing 12% (w/v) glucose, 2% (w/v) hydrolysate of deuterated biomass of *B. methylicum B-5662*, 2% (w/v) NH_4NO_3, 1% (w/v) $MgSO_4$ $7H_2O$, 2% (w/v) $CaCO_3$, 0,01% (w/v) adenine, and 0,01% (w/v) uracil. As a control was used equivalent protonated medium containing 2% (w/v) yeast protein–vitamin concentrate (PVC).

Growth conditions

The bacterium was grown in 500 ml Erlenmeyer flasks (containing 100 ml of the growth medium) for 3–4 days at 32 °C under intensive aeration on a Biorad orbital shaker ("Biorad Labs", Hungary). The bacterial growth was controlled on the ability to form individual colonies on the surface of solid (2% (w/v) agarose) media with the same ^2H_2O-content, as well as on the optical density of the cell suspension measured on a Beckman DU-6 spectrophotometer ("Beckman Coulter", USA) at λ = 540 nm in a quartz cuvette with an optical pathway length 10 mm.

Analytical determination of [^2H]inosine

Inosine was analytically determined in 10 μl of liquid culture (LC) samples on Silufol UV-254 chromatographic plates (150×150 mm) ("Kavalier", Czech Republic) using a standard set of ribonucleosides "Beckman-Spinco" (USA) in the solvent system: *n*-butanol–acetic acid–water (2:1:1, % (v/v)). Spots were eluted with 0,1 N HCl. The UV absorbance of eluates was recorded on a Beckman DU-6 spectrophotometer ("Beckman Coulter", USA) using a standard calibration plot. The level of bioconversion of the carbon substrate was assessed using glucose oxidase (EC 1.1.3.4).

Isolation of [^{2}H]inosine from LC

Samples of LC were separated on a T-26 centrifuge ("Carl Zeiss", Germany) at 2000 g for 10 min, concentrated at 10 mm Hg in a RVO-6 rotor evaporator ("Microtechna", Hungary) to half of their initial volume, and supplemented with acetone (3×5 ml). The mixture was kept for ~10 h at 4°C, and the precipitate was separated by centrifugation at 1200 g for 5 min. The supernatant was supplemented with 20 g of activated carbon and kept for 24 h at +4 °C. The water fraction was separated by filtration; the solid phase was supplemented with 20 ml 50% (v/v) EtOH solution in 25% (v/v) ammonia (1:1, (v/v)) and heated at 60°C with a reflux water condenser. After 2–3 h, the mixture was filtered and evaporated at 10 mm Hg. The product was extracted with 0,3 M ammonium–formate buffer (pH = 8,9), washed with acetone (2×10 ml), and dried over anhydrous $CaCl_2$. Inosine was crystallized from 80% (v/v) ethanol ($[\alpha]_D^{20}$ = +1,61°; output, 3,1 g/l (80%)). Inosine was finally purified by ion exchange chromatography using a calibrated column (150×10 mm) with AG50WX 4 cation exchange resin ("Pharmacia", USA). The column was equilibrated with 0,3 M ammonium–formate buffer (pH = 8,9) containing 0,045 M NH_4Cl and eluted with the same buffer under isocratic conditions (chromatographic purity, 92%). The eluate was dried in vacuum and stored in sealed ampoules at -14°C in frost camera. ^{2}H-inosine: yield – 3,1 g/l (80%); T_m = 68–70 °C; $[\alpha]_D^{20}$ = 1,61 (ethanol); R_f = 0,5; pK_a = 1,2 (phosphate buffer with pH = 6,87). UV-spectrum (0.1 N HCl): λ_{max} = 249 nm; ε_{249} = 7100 $M^{-1}{\cdot}cm^{-1}$. FAB mass spectrum (glycerol matrix, Cs^+; accelerating voltage, 5 kV; ion current – 0,6–0,8 mA): $[M + H]^+$ *m/z* (*I*, %) 273, 20% (4 atoms ^{2}H); 274, 38 % (5 atoms ^{2}H); 275, 28% (6 atoms ^{2}H); 276, 14% (7 atoms ^{2}H); $[A + H]^+$ 136, 46%; $[B + H]^+$ 138, 55%; $[B – HCN]^+$ 111, 49%; $[B – HCN]^+$ 84, 43%.

Protein hydrolysis

Dry biomass (10 g) was treated with a chloroform–methanol–acetone mixture (2:1:1, % (v/v)), evaporated in vacuum, and supplemented with 5 ml 6 N ^{2}HCl (in ^2H_2O). The ampules were kept at 110 °C for ~24 h. Then the reaction mixture was suspended in hot ^2H_2O and filtered. The hydrolysate was evaporated at 10 mm Hg. Residual ^{2}HCl was removed in an exsiccator over solid NaOH. For preparation of ^{2}H-labeled growth substrates 200 mg of raw deuteron-biomass was suspended in 200 ml 0,5 ^{2}HCl (in ^2H_2O) and autoclaved at 60 °C for ~1,5 h. The reaction mixture was neutralized with 0,5 N NaOH (in ^2H_2O) till pH = 6,5–6,7, and evaporated at 10 mm Hg. The dry residue was used for preparation of growth media.

Hydrolysis of intracellular policarbohydrates

Dry biomass (50 mg) was placed into a 250 ml round bottomed flask, supplemented with 50 ml distilled ^2H_2O and 1,6 ml 25% (v/v) H_2SO_4 (in ^2H_2O), and boiled in a reflux water evaporator for ~90 min. After cooling, the reaction mixture was suspended in one volume of hot distilled ^2H_2O and neutralized with 1 N $Ba(OH)_2$ (in ^2H_2O) to pH = 7,0. $BaSO_4$ was separated by centrifugation (1500 g, 5 min); the supernatant was decanted and evaporated at 10 mm Hg.

Amino acid analysis

The amino acids of the hydrolyzed biomass were analyzed on Biotronic LC-5001 (230×3,2 mm) column ("Eppendorf–Nethleler–Hinz", Germany) with UR-30 sulfonated styrene resin ("Beckman–Spinco", USA) as a stationary phase; the mobile phase – 0,2 N sodium–citrate buffer (pH = 2,5); the granule diameter – 25 μm; working pressure – 50–60 atm; the eluent input rate – 18,5 ml/h; the ninhydrin input rate – 9,25 ml/h; detection at λ = 570 and λ = 440 nm (for proline).

Analysis of carbohydrates

Carbohydrates were analyzed on Knauer Smartline chromatograph ("Knauer", Germany) equipped with a Gilson pump ("Gilson Inc.", USA) and a Waters K 401 refractometer ("Waters Associates", Germany) using Ultrasorb CN column (250×10 mm) as a stationary phase; the mobile phase, acetonitrile–water (75:25, % (v/v); the granule diameter – 10 μm; the input rate – 0,6 ml/min.

UV spectroscopy

The UV spectra were registered with Beckman DU-6 programmed spectrophotometer ("Beckman Coulter", USA) at λ = 220–280 nm.

FAB mass spectrometry

FAB mass spectra were recorded on VG-70 SEQ chromatograph ("Fisons VG Analytical", USA) equipped with a cesium source on a glycerol matrix with accelerating voltage 5 kV and ion current 0,6–0,8 mA.

EI mass spectrometry

EI mass spectra were recorded with MB-80A device ("Hitachi", Japan) with double focusing (the energy of ionizing electrons – 70 eV; the accelerating voltage – 8 kV; the cathode temperature – 180–200 °C) after amino acid modification into methyl esters of N-5-dimethylamino(naphthalene)-1-sulfonyl (dansyl) amino acid derivatives according to an earlier elaborated protocol.

Results and Discussion

Preparation of deutero-biomass of *B. methylicum B-3157*

For this study was used a mutant strain of the Gram-positive chemoheterotrophic bacterium *B. subtilis B-3157*, polyauxotrophic for histidine, tyrosine, adenine, and uracil (preliminary adapted to deuterium by selection of individual colonies on growth media with increased ^2H_2O content). Due to impaired metabolic pathways involved in the regulation of the biosynthesis of purine ribonucleosides, this strain under standard growth conditions (PVC-medium, late exponential growth, +32 °C) synthesizes 17–20 g of inosine per 1 liter of the LC [21].

The maximal yield of inosine was attained on a protonated medium with 12% (w/v) glucose as a source of carbon and energy and 2% (w/v) yeast PVC as a source of growth factors and amine nitrogen. In our experiments it was necessary to replace the protonated growth substrates with their deuterated analogs, as well as to use ^2H_2O of high isotopic purity. For this purpose, we used the autoclaved biomass of the Gram-positive facultative methylotrophic bacterium *B. methylicum B-5662*, capable to assimilate methanol *via* RuMP pathway of carbon assimilation. Owing to a 50–60% rate of methanol bioconversion (conversion efficiency – 15,5–17,3 gram dry biomass per 1 gram of assimilated substrate) and stable growth on deuterated minimal medium M9 with 98% (v/v) ^2H_2O and 2% (v/v) [^{2}H]methanol, this strain is the most convenient source for producing the deuterated biomass; moreover, the cost of bioconversion is mainly determined by the cost of ^2H_2O and [^{2}H]methanol [22].

The adaptation of *B. methylicum B-5662* was necessary to improve the growth characteristics of this strain and attain high output of microbial biomass on the maximally deuterated M9 medium. For this purpose, we used a stepwise increasing gradient of ^2H_2O-concentration in M9 growth media (from 24,5; 49,0; 73,5 up to 98% (v/v) ^2H_2O) in the presence of 2 % (v/v) methanol and its ^{2}H-labeled analog ([^{2}H]methanol), because we assumed that gradual cell adaptation to ^2H_2O would have a favorable effect on the growth parameters of the strain (Table 1).

Table 1: Isotopic components of growth media M9 and characteristics of bacterial growth of *B. methylicum B-5662**

Experiment number	Media components, % (v/v)				Lag-period (h)	Yield of biomass, gram from 1 l of LC	Generation time (h)
	H_2O	^2H_2O	Methanol	[^{2}H]methanol			
1	98,0	0	2	0	20±1,40	200,2±3,20	2,2±0,20
2	98,0	0	0	2	30±1,44	184,6±2,78	2,4±0,23
3	73,5	24,5	2	0	32±0,91	181,2±1,89	2,4±0,25
4	73,5	24,5	0	2	34±0,89	171,8±1,81	2,6±0,23
5	49,0	49,0	2	0	40±0,90	140,2±1,96	3,0±0,32
6	49,0	49,0	0	2	44±1,38	121,3±1,83	3,2±0,36

7	24,5	73,5	2	0	45±1,.41	112,8±1,19	3,5±0,27
8	24,5	73,5	0	2	49±0,91	94,4±1,74	3,8±0,25
9	0	98,0	2	0	58±1,94	65,8±1,13	4,4±0,70
10	0	98,0	0	2	60±2,01	60,2±1,44	4,9±0,72
10'	0	98,0	0	2	40±0,88	174,0±1,83	2,8±0,30

Notes:

* The data in Expts. 1–10 are submitted for *B. methylicum* at growing on growth media with 2% (v/v) methanol/[^{2}H]methanol and specified amounts (%, v/v) ^2H_2O. The data in Expt. 10' are submitted for adapted for maximum content of deuterium in growth medium bacterium *B. methylicum* at the growing on growth media with 2% (v/v) of [^{2}H]methanol and 98% (v/v) of ^2H_2O. As the control used experiment where used ordinary protonated water and methanol.

To study the effect of the degree of carbon source deuteration on the growth parameters of the strain, in experiments 1, 3, 5, 7, and 9 was used protonated methanol, and [^{2}H]methanol in experiments 2, 4, 6, 8, and 10 (Table 1). The results demonstrated that the replacement of protonated methanol with its deuterated analog within the same concentration of ^2H_2O in the growth media slightly decreased the growth characteristics (Table 1, experiments 2, 4, 6, 8, and 10). Therefore, in further experiments were used M9 media with ^2H_2O and [^{2}H]methanol. When the initial strain of *B. methylicum* was cultivated on protonated M9 medium with water and methanol, the duration of lag-phase and cell generation time were 20 and 2,2 h, respectively, with an output of biomass 200 gram per 1 liter of LC (Table 1, experiment 1). In the intermediate experiments (2–10), these parameters varied proportionally to the ^2H_2O concentration (Table 1). The observed effect consisted in the increase in the lag-phase period and cell generation time with a simultaneous decrease in microbial biomass outputs on media with increasing ^2H_2O-content. The most remarkable values of this parameters were detected in experiment 10, in which was used the maximally deuterated medium with 98% (v/v) ^2H_2O and 2% (v/v) [^{2}H]methanol; the lag-phase and cell generation time in these conditions were increased in 3- and 2,2-fold times, respectively, as compared to the control conditions (water and methanol; Table 1, experiment 1), and the biomass output decreased in 3,1-fold. The adaptation to deuterium (experiment 10', Table 1) permitted to improve essentially the growth characteristics of *B. methylicum B-5662* on maximally deuterated growth medium. The output of biomass produced by the adapted bacterium decreased by 13% as compared to the control with an increase in the generation time to 2,8 h and the lag phase to 40 h (experiment 10', Table 1).

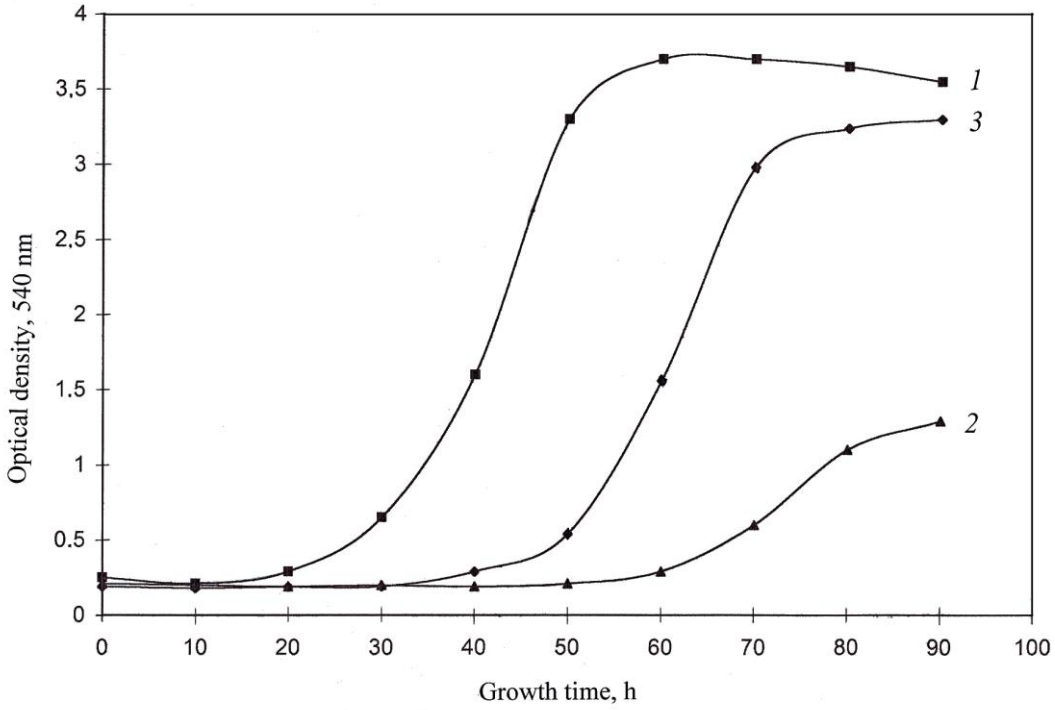

Figure 1. Growth dynamics of *B. methylicum B-5662* (1, 2, 3) on media M9 with various isotopic content: *1* – non-adapted bacterium on protonated medium M9 (Table 1, experiment 1); *2* – non-adapted bacterium on maximally deuterated medium M9 (Table 1, experiment 10); *3* – adapted to ^2H_2O bacterium on maximally deuterated medium M9 (Table 1, experiment 10')

The adaptation was monitored by recording the growth dynamics of the initial bacterium (Figure 1, curve *1*, control, protonated M9 medium) and adapted to deuterium *B. methylicum B-5662* (Figure 1, curve *3*) on the maximally deuterated M9 medium with 98% (v/v) ^2H_2O and 2% (v/v) [^{2}H]methanol. Unlike the adapted bacterium (Figure 1, curve *3*), the growth dynamics of the initial bacterium (Figure 1, curve *1*) on the maximally deuterated medium were inhibited by deuterium. Being transferred to the protonated medium, the adapted bacterium returned to normal growth after a certain lag-phase period that was characteristic for other adapted bacterial strains. The effect of growth reversion in protonated/deuterated media demonstrates that adaptation to ^2H_2O is a phenotypic phenomenon, although it cannot be excluded that a certain genotype determined the manifestation of the same phenotypic attribute in media with high deuterium content. In general, the improved growth characteristics of the adapted bacterium significantly simplify the scheme for the production of deuterated biomass, the optimal conditions for which are satisfied the following: maximally deuterated M9 medium with 98% (v/v) ^2H_2O and 2% (v/v) [^{2}H]methanol, incubation period 3–4 days, and temperature +35 ^{o}C.

The data on the yield of biomass of initial and adapted *B. methylicum*, magnitude of lag-period and generation time on the protonated and the maximumally deuterated M9 medium are shown in Figure 2. The degree of cell survive on maximum deuterated medium was approx. 40%. The yield of biomass for adapted methylotroph (*c*) was decreased approx. on 13% in comparison with control conditions (*a*) at an increase in the time of generation up to 2,8 h and the lag-period up to 40 h (Fig. 2). As is shown from these data, as compared with the adapted strain, the growth characteristics of initial strain on maximally deuterated medium were inhibited by deuterium.

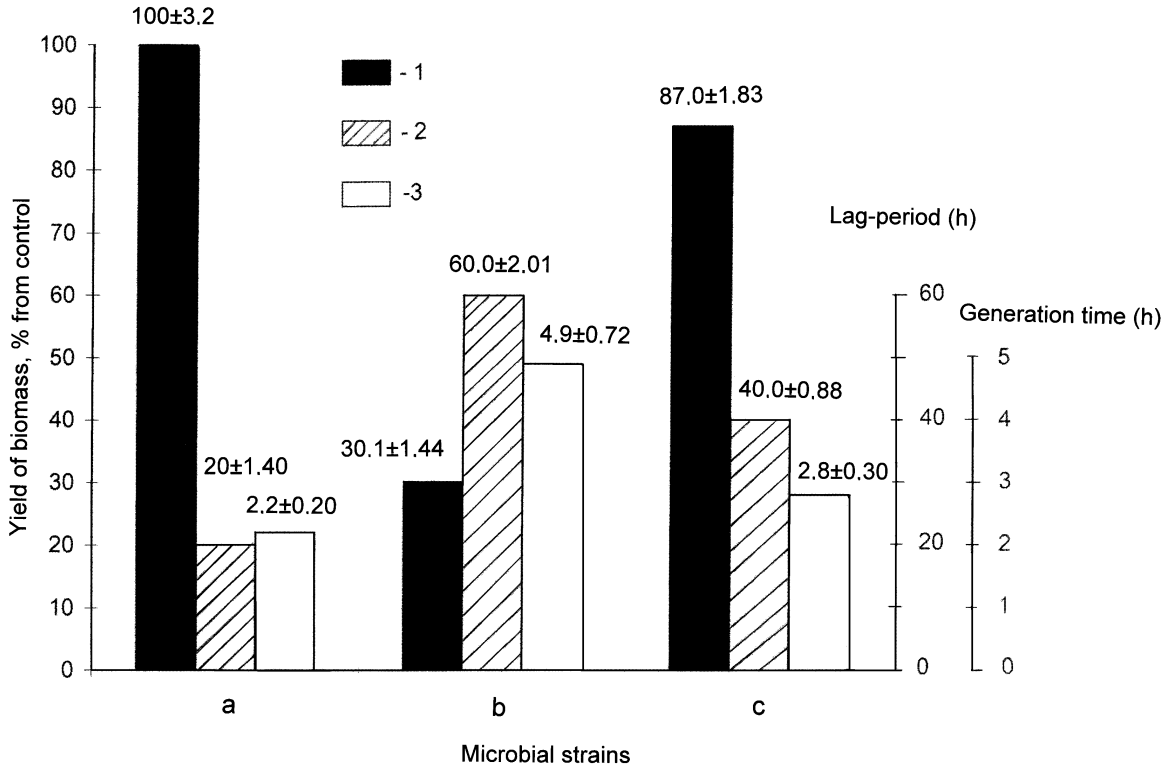

Figure 2. Yield of microbial biomass of *B. methylicum*, magnitude of lag-period and generation time in various experimental conditions: initial strain on protonated M9 medium (control) with water and methanol (*a*); initial strain on maximally deuterated M9 medium (b); adapted to deuterium strain on maximally deuterated M9 medium (c): 1 – yield of biomass, % from the control; 2 – duration of lag-period, h; 3 – generation time, h.

Biosynthesis of [^{2}H]Inosine

The strategy for the biosynthesis of [^{2}H]inosine by *B. subtilis B-3157* using the biomass of *B. methylicum B-5662* as growth substrates was developed taking into account the ability of methylotrophic bacteria to synthesize large amounts of protein (output, 50% (w/w) of dry weight), 15–17% (w/w) of polysaccharides, 10–12% (w/w) of lipids (mainly, phospholipids), and 18% (w/w) of ash [23]. To provide high outputs of these compounds and minimize the isotopic exchange (^{1}H–^{2}H) in amino acid residues of protein molecules, the biomass was hydrolyzed by autoclaving in 0,5 N ^{2}HCl (in ^2H_2O).

Since the inosine-producing strain of *B. subtilis B-3157* is a polyauxotroph requiring tyrosine and histidine for its growth, we studied the qualitative and quantitative content of amino acids in the hydrolyzed methylotrophic biomass produced in the maximally deuterated medium M9 with 98% (v/v) ^2H_2O and 2% (v/v) [^{2}H]methanol, and the levels of their deuterium enrichment (Table 2). The methylotrophic hydrolysate contains 15 identified amino acids (except for proline detected at λ = 440 nm) with tyrosine and histidine content per 1 gram of dry methylotrophic hydrolysate 1,82% and 3,72% (w/w), thereby satisfying the auxotrophic requirements of the inosine producer strain for these amino acids. The content of other amino acids in the hydrolysate is also comparable with the needs of the strain in sources of carbon and amine nitrogen (Table 2).

The indicator determining the high efficiency of deuterium incorporation into the synthesized product is high levels of deuterium enrichment of amino acid molecules, varied from 49 atom% ^{2}H for leucine/isoleucine to 97,5 atom% ^{2}H for alanine (Table 2). This allowed using the hydrolysate of deuterated biomass of *B. methylicum* as a source of growth substrates for growing the inosine-producing strain *B. subtilis*.

Table 2: Amino acid composition of hydrolyzed biomass of the facultative methylotrophic bacterium *B. methylicum B-5662* obtained on maximally deuterated M9 medium with 98% (v/v) ^2H_2O and 2% (v/v) [^{2}H]methanol and levels of deuterium enrichment*

Amino acid	Yield, % (w/w) dry weight per 1 gram of biomass		Number of deuterium atoms incorporated into the carbon backbone of a molecule**	Level of deuterium enrichment of molecules, % of the total number of hydrogen atoms***
	Protonated sample (control)	Sample from deuterated M9 medium		
Glycine	8,03	9,69	2	90,0±1,86
Alanine	12,95	13,98	4	97,5±1,96
Valine	3,54	3,74	4	50,0±1,60
Leucine	8,62	7,33	5	49,0±1,52
Isoleucine	4,14	3,64	5	49,0±1,50
Phenylalanine	3,88	3,94	8	95,0±1,85
Tyrosine	1,56	1,83	7	92,8±1,80
Serine	4,18	4,90	3	86,6±1,56
Threonine	4,81	5,51	–	–
Methionine	4,94	2,25	–	–
Asparagine	7,88	9,59	2	66,6±1,62
Glutamic acid	11,68	10,38	4	70,0±1,64
Lysine	4,34	3,98	5	58,9±1,60
Arginine	4,63	5,28	–	–
Histidine	3,43	3,73	–	–

Notes:
* The data were obtained for methyl esters of N-5-dimethylamino(naphthalene)-1-sulfonyl (dansyl) chloride amino acid derivatives.
** At calculation the level of deuterium enrichment, the protons (deuterons) at COOH- and NH_2-groups of amino acid molecules were not taken into account because of the dissociation in $H_2O/^2H_2O$.
*** A dash denotes the absence of data.

The growth and biosynthetic characteristics of the inosine-producing strain *B. subtilis B-3157* were studied on protonated yeast PVC medium with H_2O and 2% (w/v) yeast PVC and on HW medium with 89% (v/v) ^2H_2O and 2% (w/w) of hydrolysate of deuterated biomass of *B. methylicum* (Figure 3). Experiments demonstrated a certain correlation between the changes of growth dynamics of *B. subtilis B-3157* (Fig. 3, curves *1*, *1*'), output of inosine (Figure 3, curves *2*, *2*'), and glucose assimilation (Figure 2, curves *3*, *3*'). The maximal output of inosine (17 g/l) was observed on protonated PVC medium at a glucose assimilation rate 10 g/l (Figure 3, curve *2*). The output of inosine in the HW medium decreased in 4,4-fold, reaching 3,9 g/l (Figure 3, curve *2*'), and the level of glucose assimilation – 4-fold, as testified by the remaining 40 g/l non-assimilated glucose in LC (Figure 3, curve *3*'). The experimental data demonstrate that glucose is less efficiently assimilated during growth in the HW medium as compared to the control conditions in H_2O.

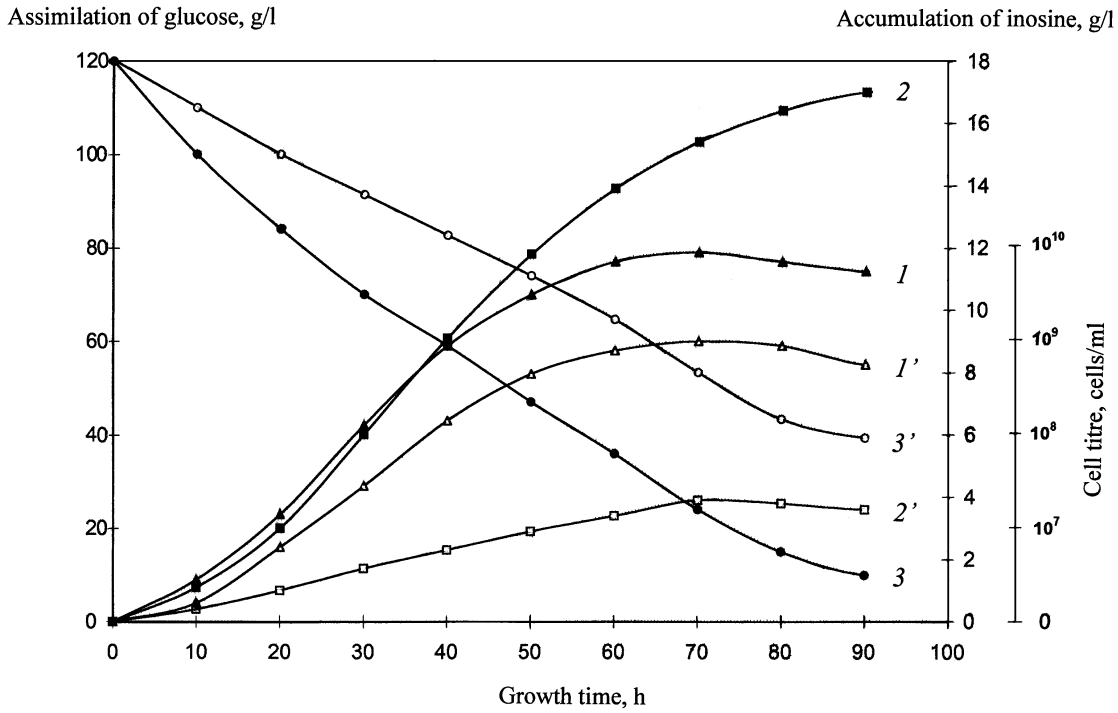

Figure 3. Growth dynamics of *B. subtilis B-3157* (*1*, *1*') (cells/ml), inosine accumulation in LC (*2*, *2*') (g/l), and glucose assimilation (*3*, *3*') (g/l) under different experimental conditions: (*1–3*) – protonated yeast PVC medium; (*1*'–*3*') – HW medium with 2% (w/v) hydrolysate of deuterated biomass of *B. methylicum B-5662*.

This result demanded the examination of the content of glucose and other intracellular carbohydrates in the biomass of the inosine-producer strain of *B. subtilis B-3157*, which was performed by reverse phase HPLC on an Ultrasorb CN column (10 μm, 10×250 mm) with a mixture of acetonitrile–water (75:25, % (v/v)) as a mobile phase (Table 3). The fraction of intracellular carbohydrates in Table 3 (numbered according to the sequence of their elution from the column) comprises monosaccharides (glucose, fructose, rhamnose, and arabinose), disaccharides (maltose and sucrose), and four unidentified carbohydrates with retention times of 3,08 (15,63% (w/w)), 4,26 (7,46% (w/w)), 7,23 (11,72% (w/w)), and 9,14 (7,95% (w/w) min (not shown). As was expected, the output of glucose in the deuterated hydrolysate was 21,4% (w/w) of dry weight, that is, higher than the outputs of fructose (6,82% (w/w)), rhamnose (3,47% (w/w)), arabinose (3,69% (w/w)), and maltose (11,62% (w/w)) (Table 3). Their outputs in microbial biomass did not differ considerably related to the control in H_2O except for sucrose, which is undetectable in the deuterated sample. The levels of deuterium enrichment in carbohydrates varied from 90,7 atom% ^2H for arabinose to 80,6 atom% ^2H for glucose.

Table 3: Qualitative and quantitative compositions of intracellular carbohydrates isolated from *B. subtilis B-3157* after growing on HW-medium and levels of the deuterium enrichment*

Carbohydrate	Content in biomass, % (w/w) of 1 g of dry biomass		Level of deuterium enrichment of molecules, %**
	Protonated sample (control)	Sample from the HW medium	
Glucose	20,01	21,40	80,6±1,86
Fructose	6,12	6,82	85,5±1,92
Rhamnose	2,91	3,47	90,3±2,12
Arabinose	3,26	3,69	90,7±3,10
Maltose	15,30	11,62	–
Sucrose	8,62	ND**	–

Notes:
* The data were obtained by IR-spectroscopy.
** ND – not detected.
*** A dash denotes the absence of data.

Isolation of [^{2}H]Inosine from the LC

The use of a combination of physical-chemical methods for isolating [^{2}H]inosine from the LC was determined by the need for preparing inosine of a high chromatographic purity (no less than 95%). Since the LC along with inosine contains inorganic salts, proteins, and polysaccharides, as well as accompanying secondary nucleic metabolites (adenosine and guanosine) and non-reacted substrates (glucose and amino acids), the LC was fractionated in a stepwise manner for isolating of [^{2}H]inosine. The high sensitivity of inosine to acids and alkali and its instability during isolation required applying diluted acid and alkaline solutions with low concentration, as well as carrying out the isolation procedure at low temperature, thus avoiding long heating of the reaction mixture. The fractionation of the LC consisted in low-temperature precipitation of high molecular weight impurities with organic solvents (acetone and methanol), adsorption/desorption on the surface of activated carbon, extraction of the end product, crystallization, and ion exchange chromatography. The proteins and polysaccharides were removed from the LC by precipitation with acetone at 4 ^{o}C with subsequent adsorption/desorbtion of total ribonucleosides on activated carbon. The desorbed ribonucleosides were extracted from the reacted solid phase by eluting with EtOH-NH_3-solution at 60 °C; inosine – by extracting with 0,3 M ammonium–formate buffer (pH = 8,9) and subsequent crystallization in 80% (v/v) EtOH. The final purification consisted in column ion exchange chromatography on AG50WX 4 cation exchange resin equilibrated with 0.3 M ammonium–formate buffer containing 0,045 M NH_4Cl with collection of fractions at R_f = 0,5. The curves *1–3* in Figure 4 shows UV-absorption spectra of inosine isolated from the LC of *B. subtilis B-3157* at various stages of isolation procedure. The presence of major absorbance band I, corresponding to natural inosine (λ_{max} = 249 nm, ε_{249} = 7100 M^{-1} cm^{-1}), and the absence of secondary metabolites II and III in the analyzed sample (Figure 4, curve *3*), demonstrates the homogeneity of isolated product and the efficiency of the isolation method.

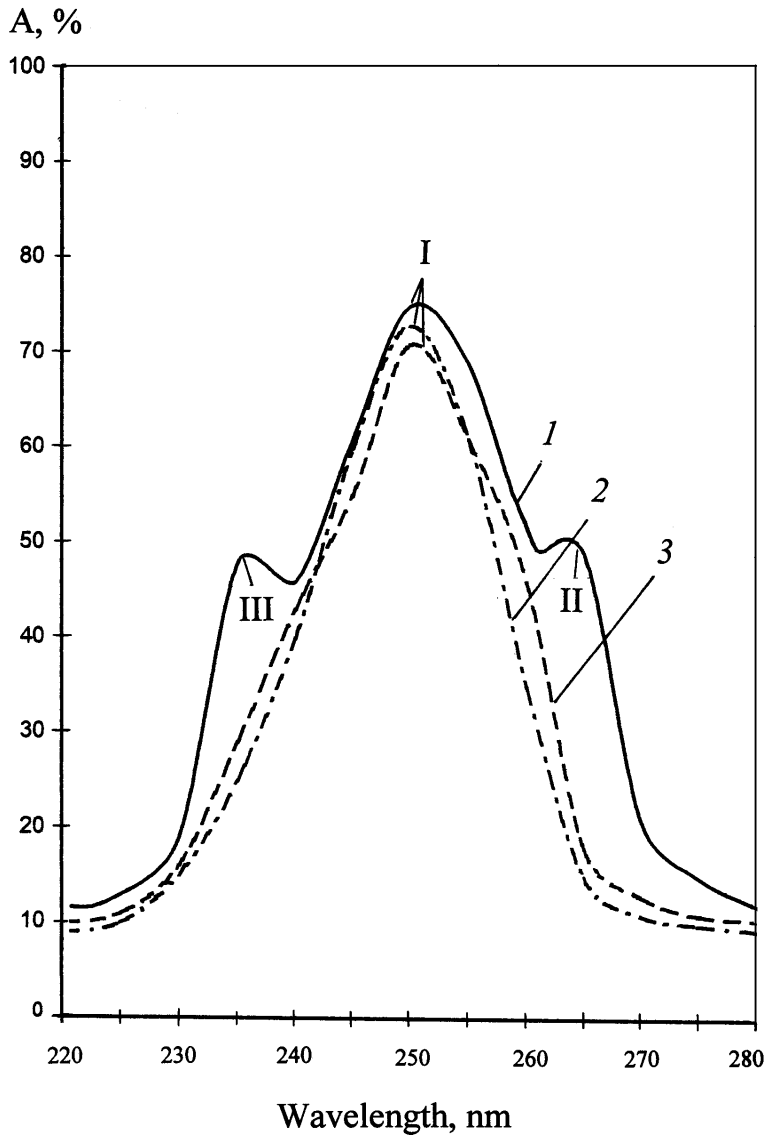

Figure 4. UV-absorption spectra of inosine (0,1 *M* HCl): (*1*) – initial LC after the growth of *B. subtilis B-3157* on HW medium; (*2*) – natural inosine; (*3*) – inosine extracted from the LC of *B. subtilis B-3157*. Natural inosine (*2*) was used as a control: (I) – inosine, (II, III) – secondary metabolites.

Studying of the level of deuterium enrichment of [^{2}H]inosine

The level of deuterium enrichment of the [^{2}H]inosine molecule was determined by FAB mass spectrometry, the high sensitivity of which allows to detect 10^{-8} to 10^{-10} moles of a substance in a sample [24]. The formation of a molecular ion peak for inosine in FAB mass spectrometry was accompanied by the migration of H^+. Biosynthetically ^{2}H-labeled inosine, which FAB mass-spectrum represented in Figure 5*b* regarding the control (natural protonated inosine, Figure 5*a*), represented a mixture of isotope-substituted molecules with different numbers of hydrogen atoms replaced by deuterium. Correspondingly, the molecular ion peak of inosine $[M + H]^+$ was polymorphically splintered into individual clusters with admixtures of molecules with statistical set of mass numbers m/z and different contributions to the total level of deuterium enrichment of the molecule. It was calculated according to the most intensive molecular ion peak (the peak with the largest contribution to the level of deuterium enrichment) recorded by a mass spectrometer under the same experimental conditions. These conditions are satisfied the most intensive molecular ion peak $[M + H]^+$ at m/z = 274 with 38% (instead of $[M + H]^+$ at m/z = 269 with 42% under the control conditions; Figure 5*a*). That result corresponds to five deuterium atoms incorporated into

the inosine molecule, obtained after growing of *B. subtilis B-3157* on HW-medium (Figure 5b). The molecular ion peak of inosine also contained less intensive peaks with admixtures of molecules containing four (m/z = 273, 20%), five (m/z = 274, 38%), six (m/z = 275, 28%), and seven (m/z = 276, 14%) deuterium atoms (Table 4).

Table 4: Values of peaks $[M+H]^+$ in the FAB mass spectra and levels of deuterium enrichment of biosynthetic inosine isolated from HW-medium

Value of peak $[M+H]^+$	**Contribution to the level of deuterium enrichment, mol.%**	**The number of deuterium atoms**	**Level of deuterium enrichment of molecules, % of the total number of hydrogen atoms***
273	20	4	20,0±0,60
274	38	5	62,5±1,80
275	28	6	72,5±1,96
276	14	7	87,5±2,98

Notes:
*At calculation of the level of deuterium enrichment, the protons(deuterons) at the hydroxyl (OH^-) and imidazole protons at NH^+ heteroatoms were not taken into account because of keto–enol tautomerism in $H_2O/^2H_2O$.

Taking into account the contribution of the molecular ion peaks $[M]^+$, the total level of deuterium enrichment (TLDE) of the inosine molecule calculated using the below equation was 65,5% of the total number of non-exchangeable hydrogen atoms in the carbon backbone of the molecule:

$$TLDE = \frac{[M]^+_{r1} \cdot C_2 + [M]^+_{r2} \cdot C_2 + ... + [M]^+_{rn} \cdot C_n}{\sum C_n}, \quad (1)$$

where $[M]^+_r$ – the values of the molecular ion peak of inosine; C_n – the contribution of the molecular ion peaks to the TLDE (mol %).

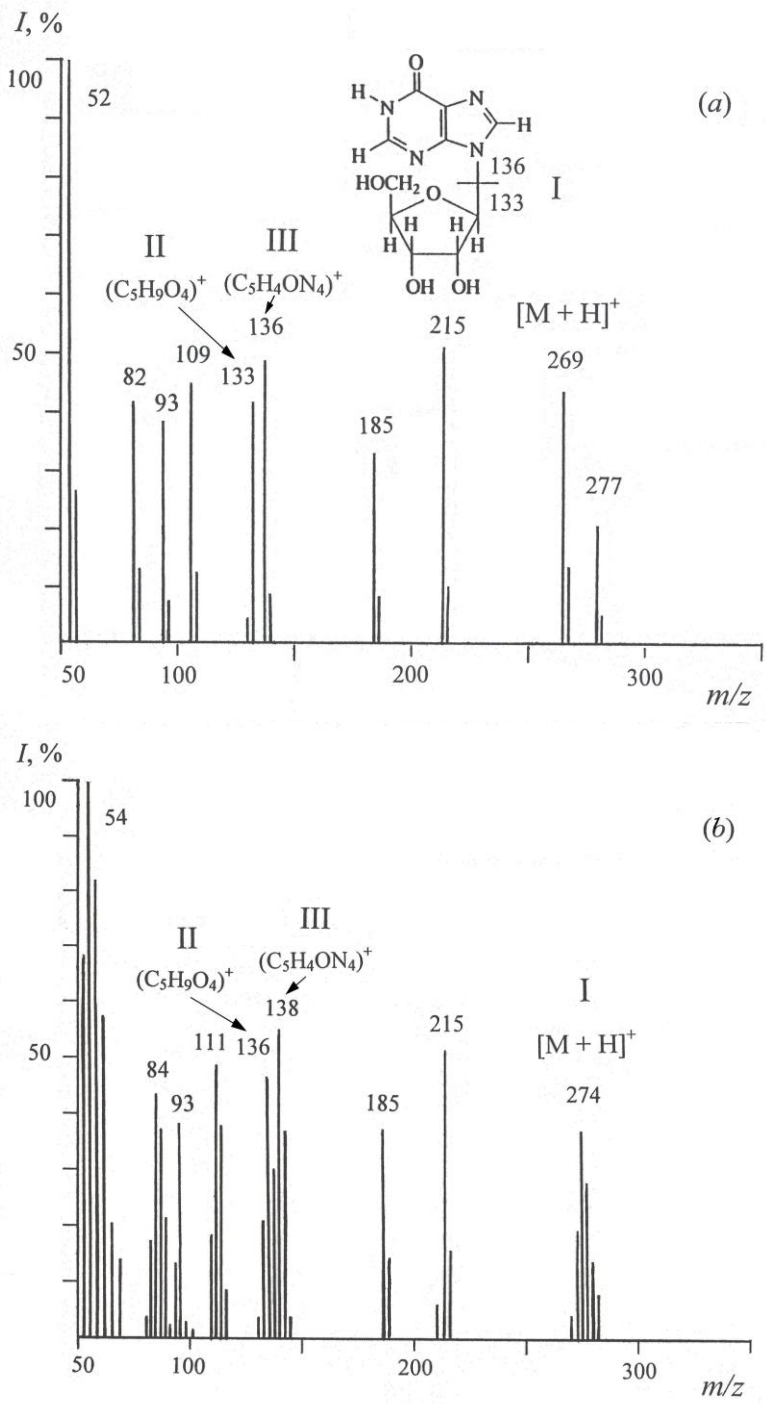

Figure 5. FAB mass spectra of inosine (glycerol as a matrix) under different experimental conditions: (*a*) – natural inosine; (*b*) – [^{2}H]inosine isolated from HW medium (scanning interval at *m/z* 50–350; major peaks with a relative intensity of 100% at *m/z* 52 and *m/z* 54; ionization conditions: cesium source; accelerating voltage, 5 kV; ion current, 0,6–0,8 mA; resolution, 7500 arbitrary units): *I* – relative intensity of peaks (%); (I) – inosine; (II) – ribose fragment; (III) – hypoxanthine fragment.

The fragmentation of the inosine molecule, shown in Figure 6, gives more precise information on the deuterium distribution in the molecule. The FAB fragmentation pathways of the inosine molecule (I) lead to formation of ribose $(C_5H_9O_4)^+$ fragment (II) at *m/z* = 133 and hypoxanthine $(C_5H_4ON_4)^+$ fragment (III) at *m/z* = 136 (their fragmentation is accompanied by the migration of H^+), which in turn, later disintegrated into several low-molecular-weight splinter fragments at *m/z*

= 109, 108, 82, 81, and 54 due to HCN and CO elimination from hypoxanthine (Figure 5). Consequently, the presence of two "heavy" fragments of ribose II $(C_5H_9O_4)^+$ at m/z = 136 (46%) (instead of m/z = 133 (41%) in the control) and hypoxanthine III $(C_5H_4ON_4)^+$ at m/z = 138 (55%) (instead of m/z = 136 (48%) in the control), as well as the peaks of low molecular weight splinter fragments formed from FAB-decomposition of hypoxanthine fragment at m/z = 111 (49%) (instead of m/z = 109 (45%) in the control) and m/z = 84 (43%) (instead of m/z = 82 (41%) in the control) suggests that three deuterium atoms are incorporated into the ribose residue, and two other deuterium atoms – into the hypoxanthine residue of the inosine molecule (Figure 5). Such selective character of the deuterium inclusion into the inosine molecule on specific locations of the molecule was confirmed by the presence of deuterium in the smaller fission fragments.

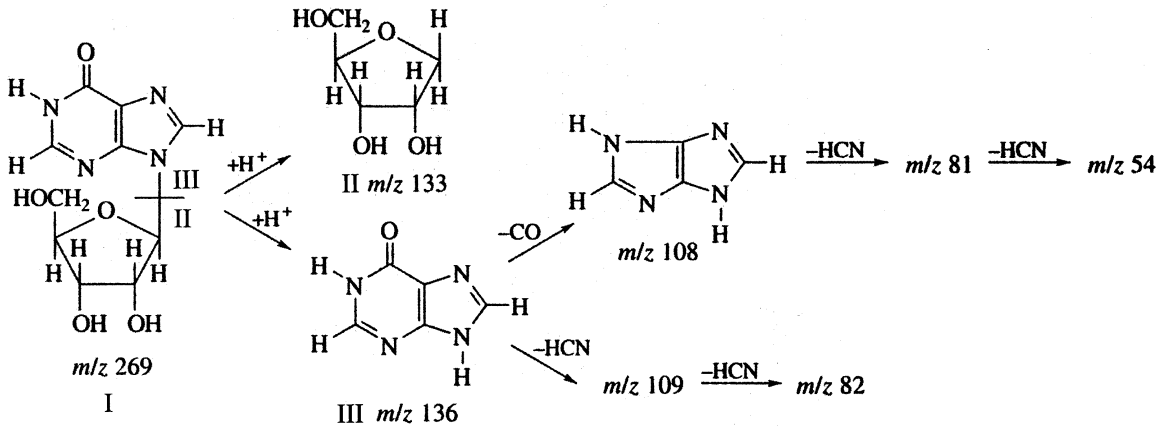

Figure 6. The fragmentation pathways of the inosine molecule leading to formation of smaller fragments by the FAB-method

The metabolic pathways of assimilation of glucose under aerobic conditions by chemoheterotrophic bacteria include the Embden-Meyerhof pathway; the anaerobic glycolysis is not widespred in this type of bacteria. When analyzing the level of deuterium enrichment of the inosine molecule we took into account the fact that the character of deuterium incorporation into the molecule is determined by the pathways of carbon assimilation (both glucose and amino acids). The carbon source was glucose as a main substrate and a mixture of deuterated amino acids from deuterated hydrolysate of methylotrophic bacterium *B. methylicum* as a source of deuterated substrates and amine nitrogen. Since the protons (deuterons) at positions of the ribose residue in the inosine molecule could have been originated from glucose, the character of deuterium inclusion into the ribose residue is mainly determined by the assimilation of glucose by glycolysis, associated with the Embden-Meyerhof pathway (Figure 7). The decomposition of glucose into two molecules of pyruvate is carried out in 10 stages, the first five of which are a preparatory stage and the next 5 – the stage interfaced with the formation of ATP. During the glycolysis glucose is phosphorylated at hydroxyl group at the sixth carbon atom (C6), forming glucose-6-phosphate (step 1). Glucose 6-phosphate is then isomerized to fructose-6-phosphate (step 2), which is phosphorylated at the hydroxyl group at the first carbon atom, with the formation of fructose 1,6-bisphosphate (step 3). During both of these reactions of phosphorylation as a donor of phosphoryl group acts ATP. Next fructose-1,6-diphosphate is split into two three-carbon molecules – glyceroldehyde 3-phosphate and dihydroxyacetone phosphate (step 4), which in the result by means of several enzymatic reactions (5–10) is converted to piruvate (Figure 7).

The overall equation of glycolysis:

$$Glucose + 2NAD^+ + 2ADP + 2P_i \rightarrow 2\ piruvate + 2NADH + 2H^+ + 2ATP + 2H_2O,$$

Most chemoheterotrophic bacteria from I group can grow under anaerobic conditions via fermentation of sugars (glycolysis), the main products of which are 2,3-butanediol, glycerol and CO_2; besides are formed minor amounts of formed lactic acid and ethanol. This type of fermentation can be represented as follows:

$$3\ mol.\ glucose \rightarrow 2,3\text{-}butanediol + 2\ mol.\ glycerol + 4\ mol.\ CO_2$$

Glucose is initially split via the Embden-Meyerhof pathway to glyceroldehyde 3-phosphate; after that there is a branching pathway. Some part of glyceroldehyde 3-phosphate is converted to dihydroxyacetone phosphate, while another part – to pyruvate, which is formed from 2,3-butanediol and CO_2. Formation of 2,3-butanediol from pyruvate leads to the re-oxidation of the NAD·H formed during the conversion of glyceroldehyde 3-phosphate to pyruvate:

2 mol. glyceroldehyde 3-phosphate + 2 mol. NAD⁺ + 4 mol. ADP + 2 mol. P → 2 mol. pyruvate + 4 mol. ATP + 2 mol. NAD·H + 2 mol. H⁺,

2 mol. pyruvate + NAD·H + H⁺ → 2 mol. CO_2 + 2,3-butanediol + NAD⁺.

The redox equilibrium is maintained by the concomitant restoration of glyceroldehyde 3-phosphate to glycerol:

Glyceroldehyde 3-phosphate + NAD·H + H⁺ → Glycerol + P + NAD⁺.

Since glucose in our experiments was used in a protonated form, its contribution to the level of deuterium enrichment of the ribose residue was neglected. However, as the investigation of deuterium incorporation into the molecule by the FAB method showed that deuterium was incorporated into the ribose residue of the inosine molecule owing to reactions of enzymatic izomerization of glucose. The numerous isotopic $^1H–^2H$ exchange processes could also have led to specific incorporation of deuterium atoms at certain positions in the inosine molecule. Such accessible positions in the inosine molecule are hydroxyl (OH^-) protons protons (C'2, C'3-positions in the ribose residue) and imidazole protons at NH^+ heteroatoms (N1-position in the hypoxanthine residue), which can be easily exchanged on deuterium in ^2H_2O *via* keto–enol tautomerism. Three non-exchangeable deuterium atoms in the ribose residue of inosine are synthesized *de novo* and could have been originated via enzymatic assimilation of glucose by the cell, while two other deuterium atoms at C2,C8-positions in the hypoxanthine residue could be synthesized *de novo* at the expense of [^2H]amino acids as glycine, glutamine and aspartate (with participation of $N^{10}–CHO–FH_4$ and $N^5,N^{10}–CH=FH_4$) (Figure 8), that originated from the deuterated hydrolysate of methylotrophic bacterium *B. methylicum* obtained on 98% of ^2H_2O medium. A glycoside proton at β-N_9-glycosidic bond could be replaced with deuterium *via* the reaction of CO_2 elimination at the stage of the ribulose-5-monophosphate formation from 3-keto-6-phosphogluconic acid with the subsequent proton (deuteron) attachment at the C1-position of ribulose-5-monophosphate. In general, our studies confirmed this scheme. However, it should be noted that auxotrophy of this mutant strain in tyrosine, histidine, adenine and uracil as well as the synthesis of a precursor of inosine, inosine-5-monophospate (IMP) from ribose-5-monophosphate and amino acids presupposes the branched metabolic pathways, different from those indicated above. It is known that intermediates in glycolysis are precursors to a number of compounds as nucleotides and amino acids. The level of deuterium enrichment of the inosine molecule is determined by isotopic purity of ^2H_2O and deuterated substrates and, therefore, for the total administration of the deuterium label into the inosine molecule instead of protonated glucoce it must be used its deuterated analogue. Deuterated glucose may be isolated in gram-scale quntities from deuterated biomass of the methylotrophic bacterium *B. methylicum*.

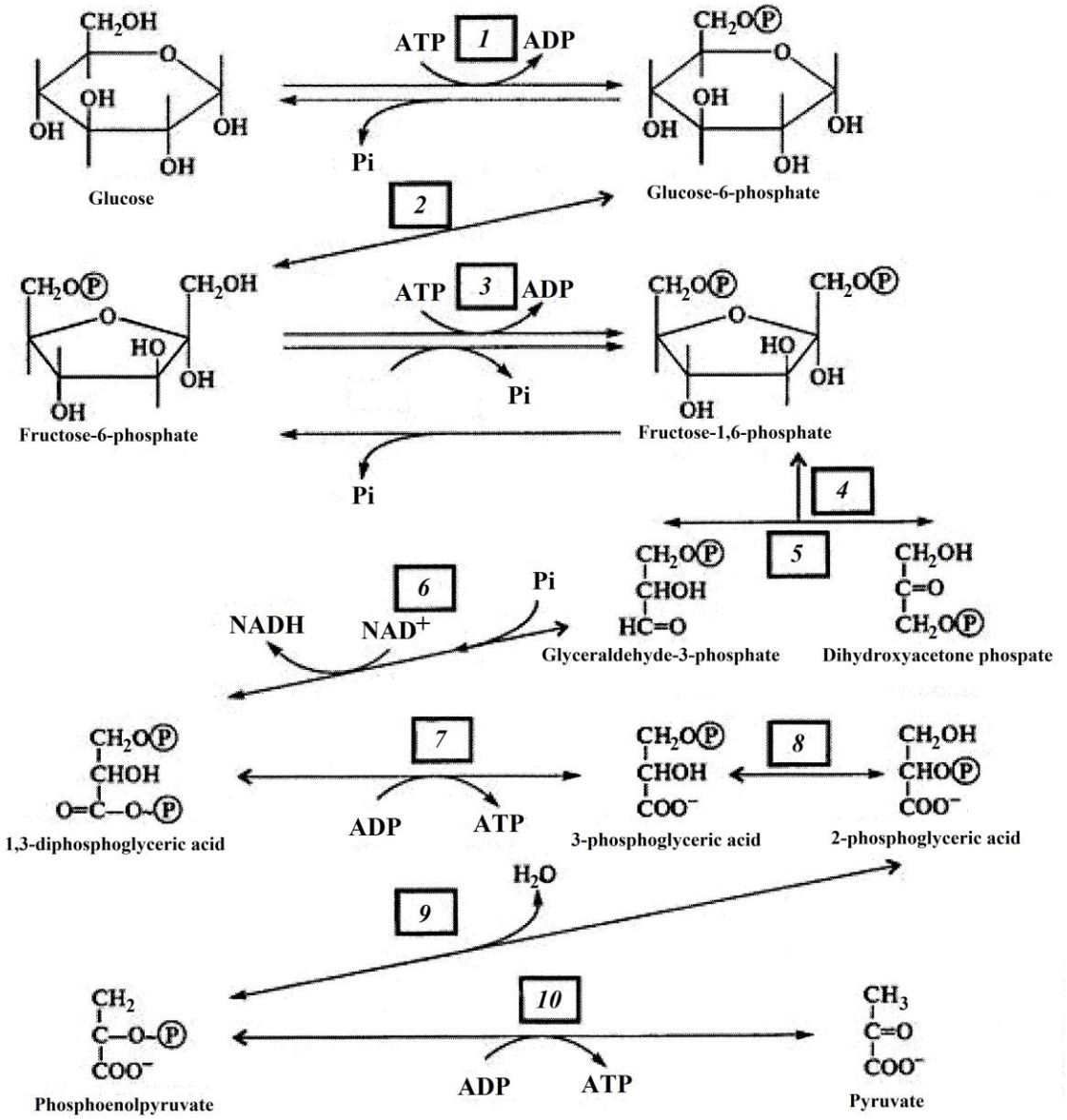

Figure 7. The Embden-Meyerhof pathway of glycolysis: 1 – hexokinase; 2 – glucose-6-phosphate izomerase; 3 – phosphofructokinase-1; 5 – fructose-1,6-bisphosphate aldolase; 6 – triosephosphate isomerase; 7 – glyceraldehyde-3-phosphat dehydrogenase; 8 – phosphoglycerate kinase; 9 – phosphoglycerate mutase; 10 – enolase; 11 – pyruvate kinase. Total reaction: Glucose + $2NAD^+$ + $2ADP + 2P_i \rightarrow$ 2 piruvate + $2NADH + 2H^+ + 2ATP + 2H_2O$ (adapted from Stryer R.Y, 1985 [25])

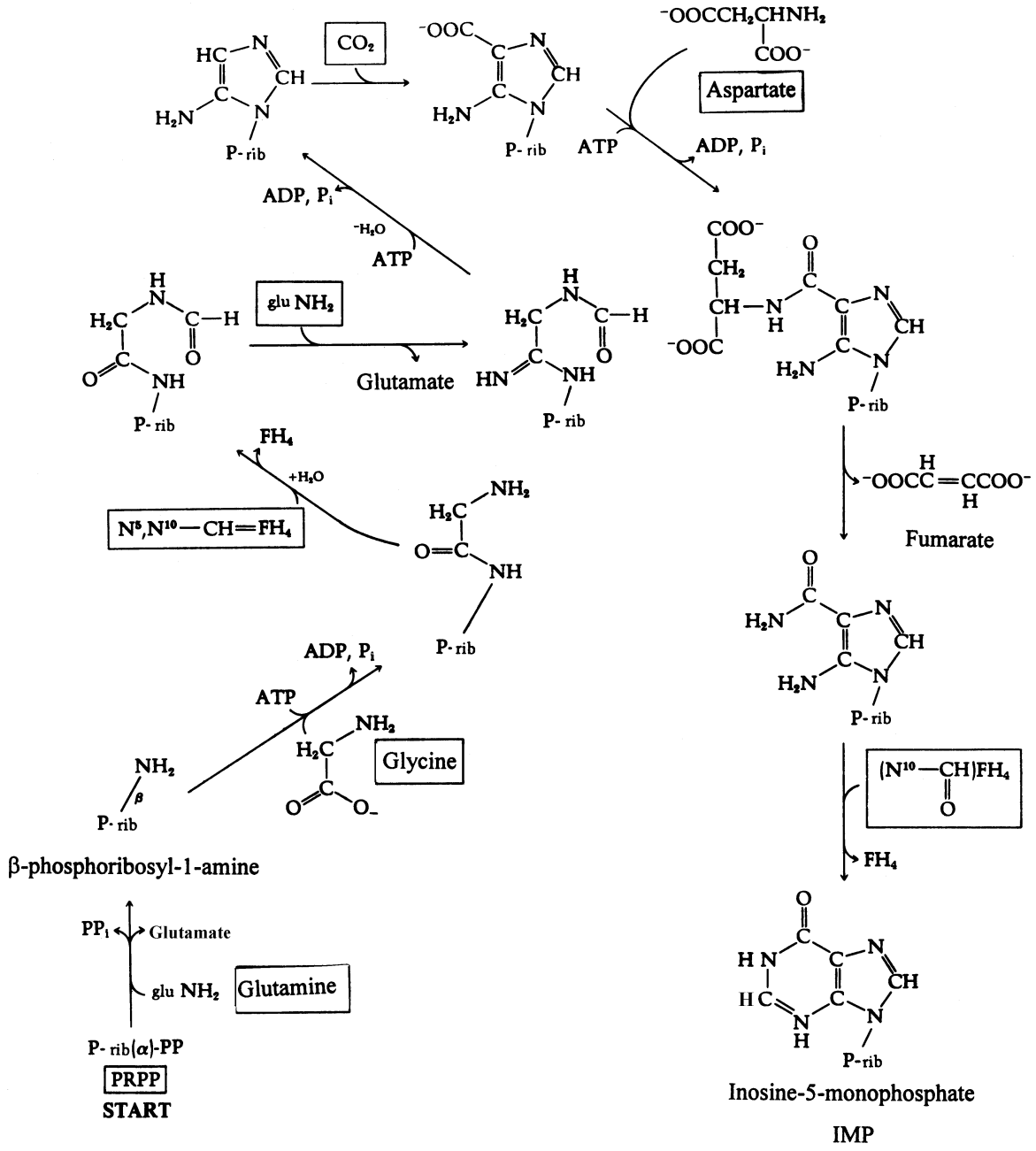

Figure 7. Overall scheme of biosynthesis of IMP in microbial cell (adapted from Bohinski, 1983 [26])

Our experiments demonstrated that chemo-heterotrophic metabolism does not undergo significant changes in ^2H_2O. This testifies about a phenotypic nature of adaptation to ^2H_2O phenomenon as the adapted cells eventually return back to the normal growth after some lag-period after their replacement back onto H_2O-medium. However, the effect of reversion of growth on $H_2O/^2H_2O$ media does not exclude an opportunity that a certain genotype determines the manifestation of the same phenotypic attribute in ^2H_2O-media with high deuterium content. At placing a cell onto ^2H_2O-media lacking protons, not only ^2H_2O is removed from a cell due to isotopic ($^1H-^2H$) exchange, but also there are occurred a rapid isotopic ($^1H-^2H$) exchange in hydroxyl (-OH), sulfohydryl (-SH) and amino (-NH_2) groups in all molecules of organic substances, including proteins, nucleic acids, carbohydrates and lipids. It is known, that in these conditions only covalent C–H bond is not exposed to isotopic ($^1H-^2H$) exchange and, thereof only molecules

with bonds such as C–^{2}H can be synthesized de novo. Thus, the most sensitive to replacement of H on ^{2}H are the apparatus of biosynthesis of macromolecules and a respiratory chain, i.e., those cellular systems using high mobility of protons and high speed of breaking up of hydrogen bonds. Last fact allows consider adaptation to ^2H_2O as adaptation to the nonspecific factor affecting simultaneously the functional condition of several numbers of cellular systems: metabolism, ways of assimilation of carbon substrates, biosynthetic processes, and transport function, structure and functions of macromolecules [27].

Conclusion

We have demonstrated the feasibility of using the FAB method for studying the biosynthetic pathways of biosynthisis of ^{2}H-labeled inosine by the bacterium *Bacillus subtilis B-3157* and evaluation of deuterium incorporation into the inosine molecule. For this aim [^{2}H]inosine was isolated from HW-medium by adsorption/desorption on activated carbon, extraction by 0,3 M ammonium–formate buffer (pH = 8,9), crystallization in 80% (v/v) EtOH, and IEC on AG50WX 4 cation exchange resin equilibrated with 0,3 M ammonium–formate buffer and 0,045 M NH_4Cl with output 3,9 g/l. The total level of deuterium enrichment of the inosine molecule was 5 deuterium atoms (65,5 atom% ^{2}H). From total 5 deuterium atoms in the inosine molecule, 3 deuterium atoms were localized in the ribose residue, while 2 deuterium atoms – in the hypoxanthine residue of the molecule. Deuterium was incorporated into the ribose residue of the inosine molecule owing to reactions of enzymatic izomerization of glucose in ^2H_2O-medium. Three non-exchangeable deuterium atoms in the ribose residue of inosine were synthesized *de novo* and originated from HMP shunt reactions, while two other deuterium atoms at C2,C8-positions in the hypoxanthine residue could be synthesized *de novo* from [^{2}H]amino acids, that originated from deuterated hydrolysate of *B. methylicum B-5662* obtained on 98% of ^2H_2O medium. To attain higher deuterium enrichment level of the final product, it is necessary to thoroughly control the isotope composition of the growth medium and exclude any possible sources of additional protons, in particular, to use [^{2}H]glucose, which may be isolated from deuterated biomass of the methylotrophic bacterium *B. methylicum B-5662*.

References:

1. Andres H. Synthesis and applications of isotopically labeled compounds / U. Pleiss and R. Voges (Eds.). – New York: John Wiley & Sons, 2001. 728 p.

2. Kundu M.T. Synthetic studies to improve the deuterium labelling in nucleosides for facilitating structural studies of large RNAs by high-field NMR spectroscopy / M.T. Kundu, A. Trifonova, Z. Dinya, A. Foldes, J. Chattopadhyaya // Nucleosides, Nucleotides and Nucleic Acids. 2001. V. 20, № 4–7. P. 1333–1337.

3. Kushner D.J. Pharmacological uses and perspectives of heavy water and deuterated compounds / D.J. Kushner, A. Baker, T.G. Dunstall // Can. J. Physiol. Pharmacol. 1999. V. 77, № 2. P. 79–88.

4. Crespi H.L. Fully deuterated microorganisms: tools in magnetic resonance and neutron scattering / H.L. Crespi // in: *Synthesis and applications of isotopically labeled compounds*. Proc. 2nd Intern. Sympos. / Eds. T. Baillie, J.R. Jones. Amsterdam: Elsevier, 1989. 332 p.

5. Caire G. Measurement of deuterium oxide by infrared spectroscopy and isotope ratio mass spectrometry for quantifying daily milk intake in breastfed infants and maternal body fat / G. Caire, C.A.M. de la Barca, A.V. Bolanos, M.E. Valencia, A.W. Coward, G. Salazar, E. Casanueva // Food Nutr. Bull. 2002. V. 23, № 3. P. 38–41.

6. Mosin O.V. Mass spectrometric evaluation of the incorporation of ^{2}H and ^{13}C into amino acids of bacteria / O.V. Mosin, D.A. Skladnev, T.A. Egorova, V.I. Shvets // Bioorganic Chemistry. 1996. V. 22, № 10-11. P. 856-869.

7. Lukin M. Structure and stability of DNA containing an aristolactam II-dA lesion: implications for the NER recognition of bulky adducts / M. Lukin, C. de los Santos // Nucleosid., Nucleotid. Nucleic Acids. 2010. V. 29, № 7. P. 562–573.

8. Chirakul P. Preparation of base-deuterated 2'-deoxyadenosine nucleosides and their site-specific incorporation into DNA / P. Chirakul, J.R. Litzer, S.T. Sigurdsson // Nucleosid., Nucleotid. Nucleic Acids. 2001. V. 20, № 12. P. 1903–1913.

9. Chen B. A general synthesis of specifically deuterated nucleotides for studies of DNA and RNA / B. Chen, E.R. Jamieson, T.D. Tullius // Bioorg. & Med. Chem. Lett. 2002. V. 12. P. 3093–3096.

10. Jung M.E. Efficient synthesis of specifically deuterated nucleosides: preparation of 4′-deuteriothymidine / M.E. Jung, Y. Xu // Cheminform Abstract. 1998. V. 29, № 16. P. 235–238.

11. Daub G.H. Synthesis with stable isotopes // Stable isotopes. Proc. 3d Intern. Conference / Ed. E. R. Klein. – New York: Acad. Press, 1979. P. 3–10.

12. Huang X. An efficient and economic site-specific deuteration strategy for NMR studies of homologous oligonucleotide repeat sequences / X. Huang, P. Yu, E. LeProust, X. Gao // Nucleic Acids Res. 2006. V. 25, № 23. P. 4758–4763.

13. Miroshnikov A.I. *A new strategy for the synthesis of nucleosides: one-pot enzymatic transformation of D-pentoses into nucleosides / A.I.* Miroshnikov, R.S. Esipov, T.I. Muravyova, I.D. Konstantinova, I.V. Fateev, I.A. Mikhailopulo // Open Conf. Proc. J. 2010. V. 1. P. 98–102.

14. Mosin O.V. Biosynthesis of ^{2}H-labeled phenylalanine by a new methylotrophic mutant *Brevibacterium methylicum* / O.V. Mosin, D.A. Skladnev, V.I. Shvets // Biosci, Biotechnol., Biochem. 1999. V. 62, № 2. P. 225–229.

15. Den'ko E.I. Influence of heavy water (D_2O) on animal, plant and microorganism's cells / E.I. Den'ko // Usp. Sovrem. Biol. 1970. V. 70, № 4. P. 41–49.

16. Vertes A. Physiological effect of heavy water. Elements and isotopes: formation, transformation, distribution / A. Vertes, Ed. – Vienna: Dordrecht: Kluwer Acad. Publ., 2003. 112 p.

17. Mosin O.V. Isotope effects of deuterium in bacterial and microalgae cells at growth on heavy water (D_2O) / O.V. Mosin, I. Ignatov // Voda: Khimiya I Ecologiya. 2012. V. 3. P. 83–94.

18. Mosin O.V. Microbial synthesis of ^{2}H-labelled L-phenylalanine with different levels of isotopic enrichment by a facultive methylotrophic bacterium Brevibacterium methylicum with RuMP assimilation of carbon / O.V. Mosin, V.I. Shvets, D.A. Skladnev, I. Ignatov // Biochemistry (Moscow) Supplement Series B: Biomedical Chemistry. 2013. V. 7, № 3. P. 249–260.

19. Trotsenko Y.A. The ribulose monophosphate (Quayle) cycle: News and views // Microbial growth on C1 compounds. Proc. 8th Intern. Sympos. / Eds. M.E. Lindstrom, F.R. Tabita. Boston: Kluwer Acad. Publ., 1995. P. 24–26.

20. Mosin O.V. Microbiological synthesis of [^{2}H]inosine with high degree of isotopic enrichment by Gram-positive chemoheterotrophic bacterium *Bacillus subtilis* / O.V. Mosin, V.I. Shvez, D.A. Skladnev, I. Ignatov // Applied Biochemistry and Microbiology. 2013. V. 49. № 3. P. 255–266.

21. Mosin O.V. Biosynthesis of ^{2}H-labelled inosine by bacterium *Bacillus subtilis* / O.V. Mosin, D.A. Skladnev, V.I. Shvets // Izv. RAN. Ser. Biologicheskaja. 1999. V. 4. P. 396–402.

22. Mosin O.V. Studying of microbial synthesis of deuterium labeled L-phenylalanine by methylotrophic bacterium *Brevibacterium methylicum* on media with different content of heavy water / O.V. Mosin, V.I. Shvets, D.A. Skladnev, I. Ignatov // Russian Journal of Biopharmaceuticals. 2012. V. 4. P. 11–22.

23. Mosin O.V. Microbiological synthesis of ^{2}H-labeled phenylalanine, alanine, valine, and leucine/isoleucine with different degrees of deuterium enrichment by the Gram-positive facultative methylotrophic bacterium *Brevibacterium methylicum* // O.V. Mosin, I. Ignatov // International Journal of BioMedicine. 2013. V. 3. № 2. P. 132–138.

24. Caprioli R.M. Continuous flow fast atom bombardment mass spectrometry / R.M. Caprioli, Ed. – New York: Wiley, 1990. 125 p.

25. Stryer L. Biochemistry / L. Strayer, Ed.. V. 2. Translated from English. – M: Mir, 1985. pp. 95-105.

26. Bohinski R.C. Modern concepts in biochemistry / R.C. Bohinski, Ed. – Boston, London, Sydney, Toronto, Massachusetts: Allyn & Bacon Inc., 1983. 378 p.

27. Ignatov I. Possible processes for origin of life and living matter with modeling of physiological processes of bacterium *Bacillus subtilis* in heavy water as model system / I. Ignatov, O.V. Mosin // Journal of Natural Sciences Research. 2013. V. 3, № 9. P. 65–76.

УДК 579.871.08

Изучение биосинтеза ^{2}H-меченого пуринового рибонуклеозида инозина хемогетеротрофной бактерией *Bacillus subtilis* B-3157

[1*] Олег Викторович Мосин
[2] Игнат Игнатов

[1] Московский государственный университет прикладной биотехнологии, Российская Федерация
Старший научный сотрудник кафедры биотехнологии, канд. хим. наук.
103316, Москва, ул. Талалихина, 33
*E-mail: mosin-oleg@yandex.ru
[2] Научно-исследовательский центр медицинской биофизики (РИЦ МБ), Болгария
Профессор, доктор наук Европейской академии естественных наук (ФРГ), директор НИЦ МБ.
1111, София, ул. Н. Коперника, 32/6
E-mail: mbioph@dir.bg

Аннотация. Изучен биосинтез ^{2}H-меченого пуринового рибонуклеозида инозина, секретируемого в культуральную жидкость (КЖ) грамположительной хемогетеротрофной бактерии *Bacillus subtilis B-3157* при выращивании этой бактерии на тяжеловодородной (ТВ) среде с 2% гидролизатом дейтерированной биомассы метилотрофных бактерий *Brevibacterium methylicum B-5662* как источника ^{2}H-меченых ростовых субстратов. Выделение ^{2}H-меченого инозина из КЖ штамма-продуцента осуществлялось адсорбцией/десорбцией на поверхности активированного угля с последующей экстракцией 0,3 М аммоний формиатым буфером (pH = 8,9), кристаллизацией в 80% этаноле и ионообменной хроматографии (ИОХ) на колонке с катионнообменной смолой AG50WX 4, уравновешенной 0,3 М аммоний формиатным буфером и 0,045 М NH_4Cl. Исследование включения дейтерия в молекулу инозина методом масс-спектрометрии с бомбардировкой быстрыми атомами (ББА) продемонстрировали включение 5 атомов дейтерия в молекулу (общий уровень дейтерированности – 65,5 атом.% ^{2}H) с включением 3-х атомов дейтерия в рибозный фрагмент и 2-х атомов дейтерия – в гипоксантиновый фрагмент молекулы. Три не обмениваемые атомы дейтерия были включены в рибозный фрагмент молекулы вследствие реакций ферментативной изомеризации глюкозы в ^2H_2O-среде за счет реакций гликолиза по пути Эмбдена-Мейергофа, в то время как два других атома дейтерия при C2, C8-положениях в гипоксантиновом остатке были синтезированы из [^{2}H]аминокислот в составе дейтерированного метилотрофного гидролизата *Brevibacterium methylicum B-5662*. Ауксотрофность штамма-продуцента в тирозине, гистидине, аденине и урациле свидетельствует о наличии разветвленных метаболических путей.

Ключевые слова: ^{2}H-меченый инозин, биосинтез, метаболизм, тяжелая вода, *Bacillus subtilis*, масс-спектрометрия ББА.

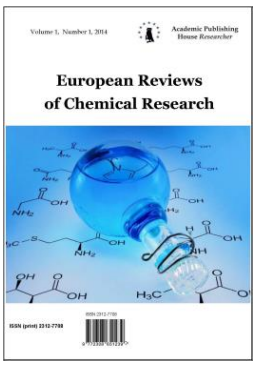

Published in the Russian Federation
European Reviews of Chemical Research
Has been issued since 2014.
ISSN: 2312-7708
E-ISSN: 2413-7243
Vol. 6, Is. 4, pp. 232-245, 2015

DOI: 10.13187/ercr.2015.6.232
www.ejournal14.com

UDC 667.62(075)

Fundamentals in Colors, Dyes and Pigments Chemistry: A Review

H.A. Shindy

Department of Chemistry, Faculty of Science,
Aswan University, Aswan, Egypt
E-mail: hashindy2@hotmail.com

Abstract

In this paper review some significant light is focused on the basis, fundamentals and/or the knowledge of colors, dyes and pigments chemistry using many of multi choice questions and their answers. This paper review is recommended for chemist's dyers and colorists. They will find it interesting, informative, stimulating, and contain a mine of information. Also, this paper review is recommended for professors and teachers in the field of colors, dyes and pigments chemistry. They can use it in teaching, as notebook/education lecturers and in their student's examination tests. In addition, this paper review can be used and/or will be most valuable in domestic and/or international scientific and/or chemistry competitions, in organic chemistry as general and particularly in the field of colors, dyes and pigments chemistry. The review covers some essential and general topics in colors, dyes and pigments chemistry, such as synthesis, properties, classification, structures, uses and applications of many aromatic and/or heterocyclic dyes. This paper review acts as a mordant and/or stabilizers for the basics, the fundamentals and/or the knowledge in understanding colors, dyes and pigments chemistry. It is considered as a special and/or specific type of collective review which has been paid little attention and is lacking in the chemistry literature.

Keywords: colors, dyes, pigments, synthesis of dyes, properties of dyes, uses of dyes, classification of dyes.

Introduction

Color will not be seen if the light is absorbed from the infrared or ultraviolet region, but if light is absorbed from the visible region, the substance will appear to be colored. If the substance absorbs all visible light except that comes ponding to yellow, for instance, it will transmit or reflect only yellow and will be seen as yellow. More commonly, however, light of only one color is absorbed, in which case the substance appears to have the complementary color. Thus if the light is absorbed from the red region, the substance will appear green [1]. When light passes through matter or is reflected from it, some of the light may be absorbed. The energy of light is transformed into the energy of motion of molecules; or electrons in the molecules may be promoted to higher energy levels. The energy is eventually transformed into heat. This implies, when matter absorbs the light energy, its temperature is raised. In rare cases, a part of light may be emitted as light of a longer wavelength, and this gives rise to phenomenon of fluorescence. The most important source of color in organic compounds is absorption of light without subsequent emission [1].

Dyes should have suitable colors. They must be able to fix themselves or be capable of being fixed to the fabric. The fixed dyes must have fastness properties such as fastness to light, resistance to the action of water, dilute acids and alkalis, and various organic solvents used in dry cleaning. There is no systematic nomenclature of dyes and many dyes have names that have been given to them by the manufactures. So it is not unusual to find a given dye having several names, and generally each dye has a trade name or names [2]. Dyes are classified according to their chemical constitution or by their application to the fiber. The former is of theoretical value to the chemists, but of little importance to the dyers, who is mainly concerned with the reaction of dyes towards the fiber being used [2].

A pigment is a material that changes the color of reflected or transmitted light as the result of wavelength-selective absorption. This physical process differs from fluorescence, phosphorescence, and other forms of luminescence, in which a material emits light. Many materials selectively absorb certain wavelengths of light. Materials that humans have chosen and developed for use as pigments usually have special properties that make them ideal for coloring other materials. A pigment must have a high tinting strength relative to the materials it colors. It must be stable in solid form at ambient temperatures. For industrial applications, as well as in the arts, permanence and stability are desirable properties. Pigments that are not permanent are called fugitive. Fugitive pigments fade over time, or with exposure to light, while some eventually blacken [3]. Pigments are used for coloring paint, ink, plastic, fabric, cosmetics, food and other materials. Most pigments used in manufacturing and the visual arts are dry colorants, usually ground into a fine powder. This powder is added to a binder (or vehicle), a relatively neutral or colorless material that suspends the pigment and gives the paint its adhesion. A distinction is usually made between a pigment, which is insoluble in its vehicle (resulting in a suspension), and a dye, which either is itself a liquid or is soluble in its vehicle (resulting in a solution). A colorant can act as either a pigment or a dye depending on the vehicle involved. In some cases, a pigment can be manufactured from a dye by precipitating a soluble dye with a metallic salt. The resulting pigment is called a lake pigment. The term biological pigment is used for all colored substances independent of their solubility [3].

Figures (1) and (2) shows the most common chromophores (color appearing and/or carriers groups) and the most common auxochromes (color deepening and/or intensifying groups), respectively. Witt (1876) was the first to show that color usually appeared in a compound when it contained a group with multiple bonds. These groups are called chromophores e.g. NO_2 (nitro), NO (nitrozo), N=N (azo), quinonoid structure, etc. [2], Figure (1). Witt also observed that certain groups which although are not chromophres, deepened the color when being introduced into a colored molecule. These groups are called auxochromes, e.g. OH (hydroxyl), NH_2 (amino), NHR (alkyl amino), NR_2 (dialkyl amino), etc. [2], Figure (2).

Certain other unsaturated groups produce color only when several of them are present in a molecule and when these are conjugated bonds e.g. C=C (ethylene), C=O (carbonyl), C=S (thiocaronyl), C=N (azomethine), etc. [1], Figure (1).

So, chromophores can be classified to strong and weak chromophores due to their strength to impart and/or introduce color to a compound. Strong chromophore (NO_2, NO, N=N) is the group which when present singly is sufficient to give color to a compound. Weak chromophore (C=C, C=O, C=S, C=N) is the group which when present singly is not able to impart color to a compound [4].

I recommend this paper [1-8] review for anyone interested in the subject, chemistry libraries and also in the personal bookshelves of every organic aromatic and/or heterocyclic dyes chemists.

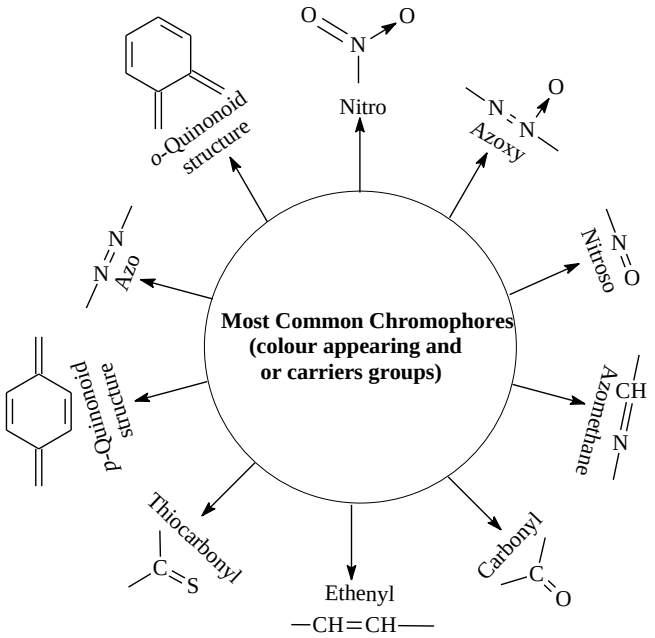

Figure (1)

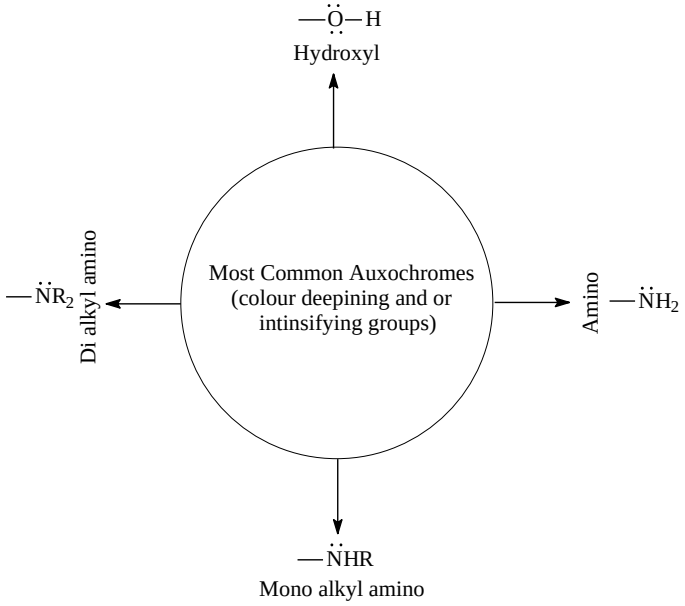

Figure (2)

Multi choice questions in colors, dyes and pigment chemistry:

1- OH group is the auxochrome in:

a- Picric acid;
b- Pinacyanol;
c- Gentian violet.

2- 1-Nitroso-2-naphthol is the scientific name of:

a- Green resorcin;

b- Green naphthol;
c- Yellow naphthol (Naphthol Yellow S).

3- Nitroso group is the chromophore in:
a- Green resorcin;
b- Yellow naphthol (Naphthol Yellow S);
c- Ethyl red.

4- 2,4-dinitroso-resorcinol is the scientific name of:
a- Orange II;
b- Acid red;
c- Green resorcin.

5- NO_2-groups are the chromophores in:
a- Chrysoidine;
b- Picric acid;
c- Kryptocyanine.

6- OH-groups are the auxochromes in:
a- Acid red;
b- Methyl orange;
c- Green resorcin.

7- Triethylorthoformate is used in the preparation of:
a- Kryptocyanine dye;
b- Ethyl red dye;
c- Apocyanine dye.

8- p-quinonoid structure is the chromophore in:
a- Orange II;
b- Green resorcin;
c- Auramine O.

9- Synthesized by coupling diazonium salt of sulphanilic acid with N,N-dimethylamino benzene:
a- Bismarck brown;
b- Methyl orange;
c- Chrysoidine.

10- OH groups are the auxochromes in:
a- Acid red dye;
b- Alizarin dye;
c- Methyl orange.

11- Prepared by condensing phthalic anhydride with catechol in the presence of concentrated H_2SO_4:
a- Alizarin;
b- Congo red;
c- Malachite green.

12- NH_2-groups are the auxochromes in:
a-Crystal violet;
b-Pararosaniline;
c-Indigotin.

13- 2,4-dinitroso-1-naphthol-7-sulphonic acid is the scientific name of:
a- Picric acid;
b- Yellow naphthol (Naphthol yellow S);
c- Orange II.

14- In acid media, methyl orange gives:
a- Two mesomeric structures;
b- Three mesomeric structures;
c- Four mesomeric structures.

15- p.quinonoid structure is the chromophore in:
a- Nitro and nitroso dyes;
b- Triarylmethane dyes;
c- Indigoid dyes.

16- $N(CH_3)_2$ groups are the auxochromes in:
a- Malachite green dye;
b- Dobener violet dye;
c- Roseaniline dye.

17- In acid media, congo red gives:
a- Two mesomeric structures;
b- Three mesomeric structures;
c- Four mesomeric structures.

18- p.quinonoid structure is the chromophore in:
a- Green resorcin;
b- Alizarin;
c- Green naphthol.

19- In acid media, methyl orange has:
a- Yellow color;
b- Red color;
c- Violet color.

20- In acid media, congo red dye gives:
a- Red color;
b- Orange color;
c- Blue color.

21- The color of phenolphthaleine in acid media is:
a- White and/or colorless;
b- Pink and/or red color;
c- Blue color.

22- Alizarin dye is used in:
a-Manufacturing of inks;
b-Coloring foods;
c-Coloring woods.

23- NH_2-groups are the auxochromes in:
a- Phenolphthaleine;
b- Congo red;
c-Erythrosine.

24- In Base media, methyl orange has:
a- Yellow color;
b- Green color;
c- Blue color.

25- Azo grop is the chromophore in:
a- Green naphthol;
b- Eosin;
c- Methyl orange.

26- Cyanine dyes are used in medicine as:
a- a laxative;
b- Antibiotics;
c- Antitumor and/or anticancer agents.

27- In base media, congo red has:
a- Red color;
b- Blue color;
c- Yellow color.

28- $N(Me)_2$ groups are the auxochromes in:
a- Methyl orange;
b- Phenolphthaleine sulphone;
c-Besmark brown.

29- The color of phenolphthaleine dye in base media is:
a- Green color;
b- White and/or colorless;
c- Pink and/or red color.

30- Azo groups are the chromophores in:

a-Indigotin dye;
b-Fluorescein dye;
c- Congo red dye.

31- 2,4-diamino-azo-benzene is the scientific name of:

a- Chrysoidine;
b- Acid Red;
c- Green resorcin.

32- NH_2-groups are the auxochromes in:

a- Bismarck brown;
b- Alizarin;
c- Phenolphthaleine.

33- Azo group is the chromophore in:

a-Fluorescein dye;
b- Chrysoidine dye;
c- Alizarin.

34- NH_2-groups are the auxochromes in:

a- Methyl orange;
b- Chrysoidine;
c- Picric acid.

35- Azo groups are the chromophores in:

a- Yellow naphthol;
b- Green naphthol;
c- Besmark brown.

36- Phenolphthaleine is used as:

a- Extremely powerful laxative;
b- Antiseptic agent;
c- anticancer agent.

37-Fluorescein is used as:

a- Anticancer agent;
b- A mild purgative;
c- Antitumor agent.

38- OH-group is the auxochrome in:

a- Orange II;
b- Crystal violet;
c- Gentian violet.

39- Azo-, Nitro- and SO_3H-groups are the chromophores in:

a- Acid red;
b- Green resorcin;
c- Orange II.

40- Chrysoidine is prepared by coupling benzene diazonium chloride (diazotized aniline) with:

a- o.phenylene diamine;
b- p.phenylene diamine;
c- m.phenylene diamine.

41- Gives orange-red color in acid media:

a- Phenolphthaleine;
b-Fluorescein.
c- Eosin.

42- NH_2 is the auxochrome in:

a- Methyl orange;
b- Acid red;
c-Erythrosine.

43- Azo- and SO_3H-group are the chromophores in:

a- Eosin;
b- Malachite green;

c- Orange II.

44- Gives strong and/or deep green color in base media:

a-Fluorescein;
b- Eosin;
c-Erythrosine.

45- OH-group is the auxochrome in:

a- Dobener violet;
b- Yellow naphthol (Naphthol Yellow S);
c- Pararosaniline.

46- Nitroso group is the chromophore in:

a- Green naphthol;
b- Acid red;
c- Bismarck brown.

47- The color of fluorescein in acid media is:

a- Green;
b- Orange-red;
c- Yellow.

48- Nitro and sulphonic groups are the chromophores in:

a- Yellow naphthol (Naphthol Yellow S);
b- Chrysoidine;
c- Green naphthol.

49- Reaction of 2 mole of 1-ethyl-quinaldinium iodide salts with triethylorthoformate in alcohol / basic solution gives:

a- 2,2-Trimethine cyanine dye;
b- 2,4-Trimethine cyanine dye;
c- 4,4-trimethine cyanine dye.

50- Reaction of 2 mole of 1-ethyl-lepidinium iodide salts with triethylorthoformate in alcohol / basic solution gives:

a- 2,4-Trimethine cyanine dye;
b- 4,4-Trimethine cyanine dye;
c- 2,2-Trimethine cyanine dye.

51- The color of fluorescein dye in base media is:

a- Red color;
b- Orange color;
c- Strong and/or deep green color.

52- Alizarin dye is:

a- 1,2-diamino anthraquinone;
b- 1,2-dihydroxy anthraquinone;
c- 1-amino-2-hydroxy anthraquinone.

53- Malachite green takes its name from:

a- Its constitution nature;
b- Its classification nature;
c- The fact that it has a deep blue-green color resembling that of the malachite (copper ore).

54- Chrysoidine dye is:

a- 2,4-diamino azo benzene;
b- 2,4-dihydroxy azo benzene;
c- 2-amino-4-hydroxy azo benzene.

55- Reaction of 2 mole of 1-ethyl-quinaldinium iodide salts with triethylorthoformate in alcohol / basic solution gives:

a- Pinacyanol;
b- Kryptocyanine;
c- Ethyl red.

56- Reaction of 2 mole of 1-ethyl-lepidinium iodide salts with triethylorthoformate in alcohol/basic solution gives:

a- Ethyl red;
b- Pinacyanol;

c- Kryptocyanine.

57- Reaction of 1-ethylquinolinium iodide salts with 1-ethylquinaldinium iodide salts in alcohol / basic solution gives:

a- Pinacyanol;
b- Ethyl red;
c- Kryptocyanine.

58- Synthesized within the fabric (i.e produced on the fibre) and may be applied to any type of fibre:

a- Ingrain dyes;
b- Disperse dyes;
c- Mordant dyes.

59- Gentian violet is used as:

a- Antitumor agent;
b- Antiseptic agent;
c-Coloring food.

60- Absorbance is due to:

a- Excitation of electron to higher energy level;
b- Emission of electron to lower energy level;
c- Fluorescence of electron.

61- Fluorescence is due to:

a- Excitation of electron to higher energy level;
b- Emission of electron to lower energy level;
c- Absorbance of electron.

62- Used as antiseptic agent:

a- Bismark brown;
b- Alizarin;
c- Gentian violet.

63- Pinacyanol sensitizes the emulsion of silver bromide to the:

a- Green region (350-600 nm);
b- Red region (350-710 nm);
c- Yellow region.

64- Ingrain dyes:

a- Synthesized within the fabric (produced on the fibre) and may be applied to any type of fibre;
b- Are those which are used in their reduced state;
c- Do not dye fibre directly, they require a mordant.

65- Kryptocyanine sensitizes the emulsion of silver bromide to the:

a- Green region (350-600 nm);
b- Red region (350-710 nm);
c- Infra-red radiation.

66- The disodium salt of Eosin has:

a- Two resonance forms;
b- Three resonance forms;
c- Four resonance forms.

67- The disodium salt of phenolphthaleine sulphone has:

a- Two resonance forms;
b- Three resonance forms;
c- Four resonance forms.

68- The disodium salt of Erythrosine has:

a- Two resonance forms;
b- Three resonance forms;
c- Four resonance forms.

69- The disodium salt of tetrabromophenolphthaleine has:

a- Two resonance forms;
b- Three resonance forms;
c- Four resonance forms.

70- The disodium salt of Mercurochrome has:
a- Two resonance forms;
b- Three resonance forms;
c- Four resonance forms.

71- Its chloride salt has four resonance structures:
a- Rhodamine B;
b- Eosin;
c-Erythrosine.

72-Fluorescein dye is:
a- Cationic dye;
b- Anionic dye;
c- Zwitter ion dye.

73- Leuco is a greek word which means:
a-Colorless and/or white;
b- Yellow;
c- Orange.

74- Monomethine cyanine dyes are also named:
a- Simple cyanine dyes;
b- Hemi cyanine dyes;
c- Styryl cyanine dyes.

75- Its disodium salt has two resonance structures:
a- Phenolphthaleine;
b-Fluorescein;
c- Eosin.

76- Its disodium salt has four resonance structures:
a- Phenolphthaleine;
b- Tetra bromophenolphthaleine;
c- Eosin.

77- Pentamethine cyanine dyes are also named:
a- Carbocyanine dyes;
b- Dicarbocyanine dyes;
c- Tricarbocyanine dyes.

78- Heptamethine cyanine dyes are also named:
a- Tricarbocyanine dyes;
b- Tetracarbocyanine dyes;
c- Pentacarbocyanine dyes.

79- The chromophores in indigotin dye are:
a- 2 C=O and/or 2 o.quinonoid charged structures;
b- Nitro and/or nitroso groups;
c- Azo- and/or SO_3H-group.

80- Its disodium salt has four resonance forms:
a- Fluorescein;
b- Phenolphthaleine sulphone;
c- Tetra bromophenolphthaleine sulphone.

81- Its disodium salt has two resonance forms:
a-Erythrosine;
b- Rhodamine B;
c- Phenolphthaleine sulphone.

82- The auxochromes in indigotin dye are :
a- 2 NH-groups;
b- 2 NH_2-groups;
c- 2 C=O-groups.

83- The chromophores in thioindigotin dye are:
a- 2 C=O and/or 2 o.quinonoid charged structure;
b- Nitro and/or nitroso groups;
c- Azo- and/or SO_3H-groups;

84-Phenolphthaleine dye is:

a- Cationic dye;
b- Anionic dye;
c- Zwitter ion dye.

85-Erythrosine dye is:

a- Anionic dye;
b- Cationic dye;
c- Zwitter ion dye.

86- The auxochromes in thioindigotin dye are:

a- 2 
b- 2 C=O.
c- 2 NH.

87- Orlon fibres are:

a- Polyamide fibres;
b- Polyester fibres;
c- Polyacrylonitrile fibres.

88- Its disodium salt has two resonance forms:

a-Erythrosine;
b- Eosin;
c- Tetrabromophenolphthaleine sulphone.

89- Its disodium salt has four resonance forms:

a- Rhodamine B;
b-Erythrosine;
c- Phenolphthaleine.

90- Eosin is:

a- Zwitter ion dye;
b- Cationic dye;
c- Anionic dye.

91- Phenolphthaleine sulphone is:

a- Cationic dye;
b- Anionic dye;
c- Zwitter ion dye.

92- Its disodium salt has four resonance forms:

a- Mercurochrome;
b- Phenolphthaleine;
c- Phenolphthaleine sulphone.

93- Tetrabromophenolphthaleine sulphone dye is:

a- Anionic dye;
b- Cationic dye;
c- Zwitter ion dye.

94- Mercurochrome is:

a- Cationic dye;
b- Anionic dye;
c- Zwitter ion dye.

95- Nylon 66 is formed via condensation polymerization reaction of hexamethylene diamine with:

a- Adipic acid;
b- Glutaric acid;
c- Malonic acid.

96- Nylon 610 is formed via condensation polymerization reaction of hexamethylene diamine with:

a- Adipic acid;
b- Sebacic acid.
c- Glutaric acid.

97- Nylon 6 is formed via self condensation of:

a- 6-amino hexanoic acid;

b- 6-amino octanoic acid;.
c- 6-amino heptanoic acid.

98- Orlon fibres are formed via polymerization of:

a- Acrylonitrile;
b- Acrylic acid;
c- Ethylene.

99- Nylon 66 is formed via polymerization condensation reaction of adipic acid with:

a- Hexamethylene diamine;
b- Heptamethylene diamine;
c- Tetramethylene diamine.

100- Nylon 610 is formed via polymerization condensation reaction of sebacic acid with:

a- Pentamethylene diamine;
b- Hexamethylene diamine;
c- Octamethylene diamine.

101- Nylon 6 is formed via self polymerization condensation reaction of:

a- 6-aminohexanoic acid;
b- 5-aminohexanoic acid;
c- 4-aminohexanoic acid.

102- Nylon 6 is formed via self polymerization condensation reaction of:

a- 6-aminohexanoic acid;
b- 6-hydroxyhexanoic acid;
c- 6-mercaptohexanoic acid.

103-The name cyanine (from the Greek Kyanos) was attributed to its:

a-Beautiful blue color;
b-Beautiful orange color;
c-Beautiful yellow color.

104-Thermochromism is the property of substance to change color due to a change in:

a-Solvent polarity.
b-Temperature.
c-pH media (hydrogen ion concentration).

105-Solvatochromism means change in the color of a substance due to a change in:

a-pH media (hydrogen ion concentration).
b-Solvent polarity.
c-Temperature.

106-Halochromism is the property of substance to change color due to a change in:

a-Temperature.
b-pH media (hydrogen ion concentration).
c-Solvent polarity.

The Answers

1- a- Picric acid.
2- b- Green naphthol.
3- a- Green resorcin.
4- c- Green resorcin.
5- b- Picric acid.
6- c- Green resorcin.
7- a- Kryptocyanine dye.
8- c- Auramine O.
9- b- Methyl orange.
10- b- Alizarin dye.
11- a- Alizarin.
12- b-Pararosaniline.
13- b- Yellow naphthol (Naphthol yellow S).
14- a- Two mesomeric structures.

15- b- Triarylmethane dyes.
16- a- Malachite green dye.
17- a- Two mesomeric structures.
18- b- Alizarin.
19- b- Red color.
20- c- Blue color.
21- a- White and/or colorles.
22- a-Manufacturing of inks.
23- b- Congo red.
24- a- Yellow color.
25- c- Methyl orange.
26- c- Antitumor and/or anticancer agents.
27- a- Red color.
28- a- Methyl orange.
29- c- Pink and/or red color.
30- c- Congo red dye.
31- a- Chrysoidine.
32- a- Bismark brown.
33- b- Chrysoidine dye.
34- b- Chrysoidine.
35- c- Bismarck brown.
36- a- Extremely powerful laxative.
37- b- A mild purgative.
38- a- Orange II.
39- a- Acid red.
40- c- m.phenylene diamine.
41- b-Fluorescein.
42- b- Acid red.
43- c- Orange II.
44- a-Fluorescein.
45- b- Yellow naphthol (Naphthol Yellow S).
46- a- Green naphthol.
47- b- Orange-red.
48- a- Yellow naphthol (Naphthol Yellow S).
49- a- 2,2-Trimethine cyanine dye.
50- b- 4,4-Trimethine cyanine dye.
51- c- Strong and/or deep green color.
52- b- 1,2-dihydroxy anthraquinone.
53- c- The fact that it has a deep blue-green color resembling that of the malachite (copper ore).
54- a- 2,4-diamino azo benzene.
55- a- Pinacyanol.
56- c- Kryptocyanine.
57- b- Ethyl red.
58- a- Ingrain dyes.
59- b- Antiseptic agents.
60- a- Excitation of electron to higher energy level.
61- b- Emission of electron to lower energy level.
62- c- Gentian violet.
63- b- Red region (350-710 nm).
64- a- Synthesized within the fabric (produced on the fibre) and may be applied to any type of fibre.
65- c- Infra-red radiation.
66- c- Four resonance forms.
67- a- Two resonance forms.
68- c- Four resonance forms.

69- a- Two resonance forms.
70- c- Four resonance forms.
71- a- Rhodamine B.
72- b- Anionic dye.
73- a-Colorless and/or white.
74- a- Simple cyanine dyes.
75- a- Phenolphthaleine.
76- c- Eosin.
77- b- Dicarbocyanine dyes.
78- a- Tricarbocyanine dyes.
79- a- 2C=O and/or 20.quinonoid charged structures.
80- a-Fluorescein.
81- c- Phenolphthaleine sulphone.
82- a- 2NH groups.
83- a- 2C=O and/or 2.0.quinonoid charged structure.
84- a- Cationic dye.
85- a- Anionic dye.
86-a- 2-S
87- c-Polyacrylonitrile fibres.
88- c- Tetrabromophenolphthaleine sulphone.
89- b-Erythrosine.
90- c- Anionic dye.
91- b- Anionic dye.
92- a- Mercurochrome.
93- a- Anionic dye.
94- b- Anionic dye.
95- a- Adipic acid.
96- b- Sebacic acid.
97- a- 6-amino hexanoic acid.
98- a- Acrylonitrile.
99- a- Hexamethylene diamine.
100- b- Hexamethylene diamine.
101- a- 6-aminohexanoic acid.
102- a- 6-aminohexanoic acid.
103-a-Beautiful Blue color.
104-b-Temperature.
105-b-Solvent polarity.
106-b-pH media (hydrogen ion concentration).

Conflict of interest:
There is no conflict of interes.

Conclusion

The developments of color theories in addition to dyes and pigments synthesis and their applications in textile and non textile multidisciplinary area is growing continuously and rabidly. Certainly, this will makes the present and/or the future of this branch of organic chemistry (color, dyes and pigments chemistry) is effective, fruitful and very bright.

Acknowledgements:

I am thankful to the Chemistry department, Faculty of Science, Aswan University, Aswan, Egypt for supporting this work.

References:

1. Bahl, A., and Bahl, B.S., Advanced organic chemistry, 2009, pp. 1139-1161, (S. Chand, Company LTD, Ram Nagar, New Delhi-110 055).

2. Finar I.L., Organic Chemistry, The fundamental principles, 1990, Volume 1, sixth edition, pp. 868-899.

3. Pigment-Wikipedia, the free encyclopedia: http://en.wikipedia.org/wiki/pigment (accessed July, 20, 2015).

4-Mehta, B., Mehta, M., Organic Chemistry, PHI Learning Private Limited, New Delhi 110020, 2009, Fourth printing, pp. 1029-1049.

5. Shindy, H.A., Basics, Mechanisms and Properties in the Chemistry of Cyanine Dyes: A Review Paper, Mini-Reviews in Organic Chemistry, 2012, 9 (4), pp. 352-360.

6. Shindy, H.A., Multi Choice Questions and their Answers in Color, Dyes and Pigments Chemistry: A Review Paper, Mini-Reviews in Organic Chemistry, 2012, 9 (4), pp. 361-373.

7. David M. Sturmer (Eastman Kodak Company), Cyanine dyes in ECT (online), December, 4, 2000, pp. 1-22.

8. Thermochromism-Wikipedia, the free encyclopedia: http://en.wikipedia.org/ wiki/thermochromism (accessed August, 8, 2015).